

Final Answers to Self-Tests and Exercises

To accompany *Inorganic Chemistry*, 7th ed. by Weller, Rourke, Overton and Armstrong

Full answers and detailed explanations can be found in Solution Manual to Accompany Inorganic Chemistry, 7th ed. By Hadzovic

Chapter 1

Self-Tests

- 1.1** a) $\lambda = 1.28 \times 10^{-6}$ m or 1280 nm.
b) $n_2 = 3$.
- 1.2** a) 3d set of orbitals with five orbitals.
b) $n = 5, l = 3$; there are seven orbitals.
- 1.3** a) Four radial nodes.
b) 4p.
- 1.4** 3p.
- 1.5** a) $\sigma = 8.95$.
b) $Z_{\text{eff}} = 6.1$.
- 1.6** a) The s electron already present in Li repels the incoming electron more strongly than the p electron already present in B repels the incoming p electron, because the incoming p electron goes into a new orbital.
b) Al atoms contain one extra filled electronic shell of eight electrons ($2s^2 2p^6$) that shield the outermost electrons from the full nuclear charge.
- 1.7** a) Ni: $1s^2 2s^2 2p^6 3s^2 3p^6 3d^8 4s^2$ or $[\text{Ar}]3d^8 4s^2$ and
Ni²⁺: $1s^2 2s^2 2p^6 3s^2 3p^6 3d^8$ or $[\text{Ar}]3d^8$.
b) Cu: $1s^2 2s^2 2p^6 3s^2 3p^6 3d^{10} 4s^1$ or $[\text{Ar}]3d^{10} 4s^1$;
Cu⁺: $1s^2 2s^2 2p^6 3s^2 3p^6 3d^{10}$ or $[\text{Ar}]3d^{10}$ and
Cu²⁺: $1s^2 2s^2 2p^6 3s^2 3p^6 3d^9$ or $[\text{Ar}]3d^9$.
- 1.8** a) Period 4, Group 2, s block; Ca.
b) Period 5, Group 6, d block; Mo.
- 1.9** a) The principal quantum number, n , is lower for the electron removed from F (n

= 2), so this electron is bound more strongly than a 3p electron in Cl.

b) Ionization of Mg removes more table 3s electron.

1.10 Group 14.

1.11 a) An additional electron is added to the empty 2p orbital of C; all 2p orbitals of N are already half occupied, so an additional electron would experience sufficiently strong interelectronic repulsions.

b) A new electron would occupy completely new electronic shell that are well shielded from the nucleus and are consequently very weakly bound making an electron gain for all these elements endothermic.

1.12 a) Na⁺.

b) NaI.

Exercises

- 1.1** $E(\text{He}^+)/E(\text{Be}^{3+}) = 0.25$.
- 1.2** a) At nucleus.
b) $r = a_0$ (Borh's radius).
c) $3 + \sqrt{5}a_0$.
- 1.3** $E(\text{H}, n = 1) - E(\text{H}, n = 6) = 13.6 \text{ eV} - 0.378 \text{ eV} = 13.2 \text{ eV}$.
- 1.4** 0.544 eV. The discrepancy is due to the shielding effect.
- 1.5** $I_1(\text{Kr}) = 14.0 \text{ eV}$; $I_1(\text{Rb}) = 4.16 \text{ eV}$.
- 1.6** $\lambda = 102.5 \text{ nm}$; $E = 1.937 \times 10^{-18} \text{ J}$.

1.7 $1/\lambda = 1.524 \times 10^{-3} \text{ nm}^{-1}$, $\lambda = 656.3 \text{ nm}$.

1.8 $\frac{1}{\lambda} = R \left(\frac{1}{1^2} - \frac{1}{\infty^2} \right) = 1.0974 \times 10^7 \text{ m}^{-1}$;

$\frac{1}{\lambda} = R \left(\frac{1}{1^2} - \frac{1}{4^2} \right) = 1.0288 \times 10^7 \text{ m}^{-1}$;

$\frac{1}{\lambda} = R \left(\frac{1}{1^2} - \frac{1}{3^2} \right) = 9.7547 \times 10^6 \text{ m}^{-1}$;

$\frac{1}{\lambda} = R \left(\frac{1}{1^2} - \frac{1}{2^2} \right) = 8.2305 \times 10^6 \text{ m}^{-1}$.

1.9 $l = 0, 1, \dots, n - 1$.

1.10 n^2 (e.g., $n^2 = 1$ for $n = 1$, $n^2 = 4$ for $n = 2$, etc.)

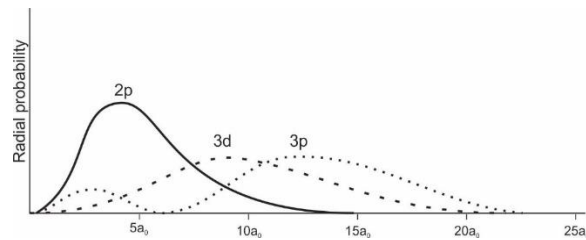
1.11

n	l	m_l	Orbital designation	Number of orbitals
2	1	+1, 0, -1	2p	3
3	2	+2, +1, ..., -2	3d	5
4	0	0	4s	1
4	3	+3, +2, ..., -3	4f	7

1.12 $n = 5$, $l = 3$ and $m_l = +3, +2, -1, 0, -1, -2, -3$.

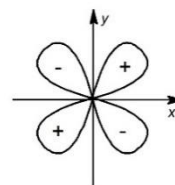
1.13 The radial distribution function is $P(r) = r^2 R^2$ (for the s orbitals this expression is the same as $4\pi r^2 \psi^2$). The plot of $r^2 R^2$ vs. r for a 1s orbital in Figure 1.10 is a radial distribution function. Figure 1.12 provides plots of the radial distribution functions for the hydrogenic 2s and 2p orbitals.

1.14 A 3p orbital has a local maximum closer to the nucleus:

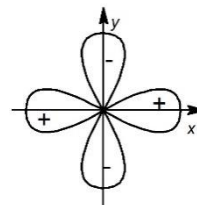


1.15 Each 4p orbital has one nodal plane; the total number of nodes is 3.

1.16 d_{xy} : function $xyR(r)$, label: xy



$d_{x^2-y^2}$: function $\frac{1}{2}(x^2 - y^2)R(r)$, label $x^2 - y^2$



1.17 In Be atom the 1s electrons shield the 2s electrons from the positive charge, which are further out from the nucleus than the 1s electrons.

1.18 Li: 1.70; Be: 2.05; B: 2.40; C: 2.75; N: 3.10; O: 3.45; F: 3.80; the trend is as expected.

1.19 The higher value of I_2 for Cr is a consequence of the special stability of half-filled subshell configurations and the higher Z_{eff} of a 3d electron vs. a 4s electron.

1.20 Both have an electron configuration that ends with $4s^2$ but zinc has 30 protons while calcium has 20, so Zn has a higher nuclear charge. However it is *effective* nuclear charge that directly affects the ionization energy of an atom. Since $I(\text{Zn}) > I(\text{Ca})$, then $Z_{\text{eff}}(\text{Zn}) > Z_{\text{eff}}(\text{Ca})$.

1.21 The first ionization energies of Sr, Ba, and Ra are 5.69, 5.21, and 5.28 eV. Ra has a higher I_1 because it has a large Z_{eff} due to the insertion of the lanthanides.

1.22 Both I_1 and I_2 remove electrons from the 4s orbital of these atoms, with the exception of Cr. In general, the 4s electrons are poorly shielded by the 3d electrons, so $Z_{\text{eff}}(4s)$ increases from left to right and I_2 also increases from left to right.

- 1.23**
- C: $[\text{He}]2s^22p^2$
 - F: $[\text{He}]2s^22p^5$
 - Ca: $[\text{Ar}]4s^2$
 - Gd^{3+} : $[\text{Ar}]3d^{10}$
 - Bi: $[\text{Xe}]4f^{14}5d^{10}6s^26p^3$
 - Pb^{2+} : $[\text{Xe}]4f^{14}5d^{10}6s^2$.

- 1.24**
- Sc: $[\text{Ar}]3d^14s^2$
 - V^{3+} : $[\text{Ar}]3d^2$
 - Mn^{2+} : $[\text{Ar}]3d^5$
 - Cr^{2+} : $[\text{Ar}]3d^4$
 - Co^{3+} : $[\text{Ar}]3d^6$
 - Cr^{6+} : $[\text{Ar}]$ or $[\text{Ar}]3d^0$
 - Cu: $[\text{Ar}]3d^{10}4s^1$
 - Gd^{3+} : $[\text{Xe}]4f^7$.

- 1.25**
- W: $[\text{Xe}]4f^{14}5d^46s^2$
 - Rh^{3+} : $[\text{Kr}]4d^6$
 - Eu^{3+} : $[\text{Xe}]4f^6$
 - Eu^{2+} : $[\text{Xe}]4f^7$
 - V^{5+} : $[\text{Ar}]$ or $[\text{Ar}]3d^0$
 - Mo^{4+} : $[\text{Kr}]4d^2$.

- 1.26**
- S
 - Sr
 - V
 - Tc
 - In
 - Sm.

1.27 See Figure 1.22 and the inside front cover of the book.

1.28 In general, I_1 , E_a , and χ increase from left to right across period 3. The cause of the general increase across the period is the gradual increase in Z_{eff} , caused by the incomplete shielding of electrons of a given value of n by electrons with the same n .

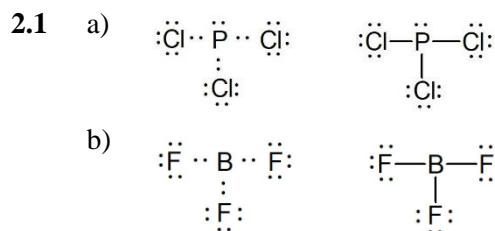
1.29 The reason is lanthanoid contraction.

1.30 2s and 2p.

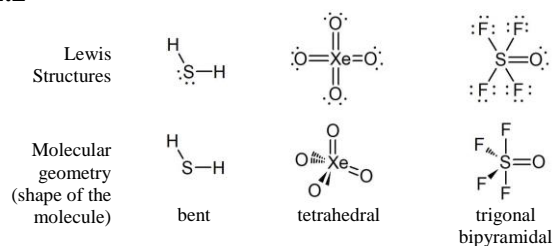
1.31 Take the data from the tables, convert them from J/mol to eV and plot them; you will see an almost linear trend that mimics Pauling's scale; there are two significant outliers from the linearity.

Chapter 2

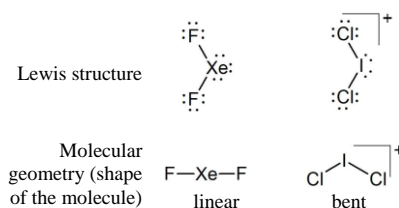
Self-Tests



2.2



2.3

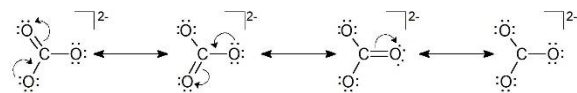


- 2.4 a) 2, 1 and 0
 b) S_2^{2-} : $1\sigma_g^2 2\sigma_u^2 3\sigma_g^2 1\pi_u^4 2\pi_g^4$
 Cl_2^- : $1\sigma_g^2 2\sigma_u^2 3\sigma_g^2 1\pi_u^4 2\pi_g^4 4\sigma_u^1$.
- 2.5 $1\sigma^2 2\sigma^2 3\sigma^2 1\pi^4 2\pi^4$.
- 2.6 a) 3
 b) 0.
- 2.7 $C\equiv N$ (shortest) < $C=N$ < $C-N$
 $C\equiv N$ (strongest) > $C=N$ > $C-N$.
- 2.8 a) $\Delta_f H(HF) = -539 \text{ kJ mol}^{-1}$.
 b) $\Delta_f H(H_2S) = 24 \text{ kJ mol}^{-1}$.
- 2.9 a) BeF_2 : ionic bonding
 b) NO: covalent bonding.

Exercises

- 2.1 a) $:N\equiv O: \overset{+}{|}$
 b) $:\ddot{Cl}-\ddot{O}: \overset{-}{|}$
 c) $H-\ddot{O}-\ddot{O}-H$
 d) $\begin{array}{c} :\ddot{Cl}: \\ | \\ :\ddot{Cl}-C-\ddot{Cl}: \\ | \\ :\ddot{Cl}: \end{array}$
 e) $\begin{array}{c} H-\ddot{O}: \\ | \\ :O: \\ | \\ S=\ddot{O}: \\ | \\ :O: \end{array}$

2.2



- 2.3 a) Bent
 b) Tetrahedral
 c) Tetrahedral.
- 2.4 a) Trigonal planar

- b) Trigonal pyramidal
 c) Square pyramidal.

- 2.5 a) Octahedral
 b) T-shaped
 c) Square pyramidal.
- 2.6 a) T-shaped
 b) Square planar
 c) Linear.
- 2.7 ICl_6^- .
- 2.8 PCl_4^+ tetrahedral; PCl_6^- octahedral.
- 2.9 a) 176 pm
 b) 217 pm
 c) 221 pm.
- 2.10 From Table 2.7, the trends in covalent radii follow closely the trends in atomic and ionic radii covered in Chapter 1 Section 1.7(a); the atomic radii decrease while the Z_{eff} increases from left to right; down the group atomic radii increase and the increase in single bond covalent radii is expected.
- 2.11 $2(Si-O) - (Si=O) = 292 \text{ kJ}$
 Therefore two single bonds will always be better enthalpically than one double bond.
- 2.12 If N_2 were to exist as N_4 molecules with the P_4 structure, then two $N\equiv N$ triple bonds would be traded for six $N-N$ single bonds, which are weak. The net enthalpy change can be estimated to be 912 kJ. The net enthalpy change for $2P_2 \rightarrow P_4$ can be estimated to be -244 kJ.
- 2.13 $\Delta H = -483 \text{ kJ mol}^{-1}$. Table 2.8 contains average bond enthalpies.
- 2.14 The atoms that obey the octet rule are O in BeO , F in NF , and O in O_2 . For the table follow the trends: bond enthalpy increases as bond order increases, and bond length decreases as bond order increases to rationalize the values.

2.15 For S_4^{2-} 0 kJ mol⁻¹, for O_4^{2-} 205 kJ mol⁻¹.

- 2.16 a) S: +4
 b) N: +3
 c) Cr: +6
 d) V: +5
 e) P: +5

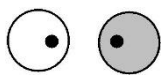
2.17 AD (least covalent) < BD < AC < AB.

- 2.18 a) BCl₃: covalent
 b) KCl: ionic
 c) BeO: ionic.

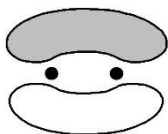
- 2.19 a) BCl₃ sp²
 b) NH₄⁺ sp³
 c) SF₄ sp³d or spd³
 d) XeF₄ sp³d².

- 2.20 a) 1
 b) 1
 c) 0
 d) 2.

2.21 a) Be₂⁺: 1σ_g²1σ_u¹



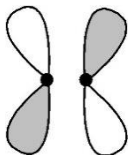
b) B₂⁻: 1σ_g²1σ_u²1π_u³



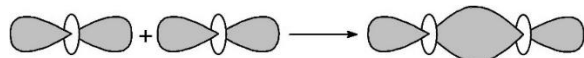
c) C₂⁻: 1σ_g²1σ_u²1π_u⁴2σ_g¹



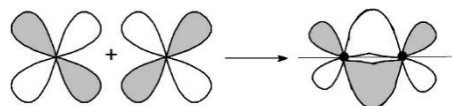
d) F₂⁺: 1σ_g²1σ_u²2σ_g²1π_u⁴1π_g³



2.22 Sigma interaction:



π interaction:



2.23 The configuration for C₂²⁻ is 1σ_g²1σ_u²1π_u⁴2σ_g² with bond order 3 and HOMO is in a sigma bonding orbital.

The configuration for C₂ is 1σ_g²1σ_u²1π_u⁴ with bond order 2.

2.24 See Figure 2.19

2.25 Similar to Figure 2.22, MO diagram for CO, with N orbitals lower in energy than B orbitals. Configuration is 1σ²2σ²1π⁴.

2.26 a) The 5p and 5s of I, and the 4p and 4s of Br.
 b) 1.

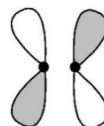
2.27 a) S₂ bond order 2, consistent with Lewis theory
 b) Cl₂ bond order 1, consistent with Lewis theory
 c) NO⁺ bond order 3, consistent with Lewis theory

2.28 a) increase from 2 to 2.5
 b) decrease from 3 to 2.5
 c) increase from 2.5 to 3.

2.29 For C₂²⁻ and N₂ HOMO:



and LUMO



For CO see Figure 2.23

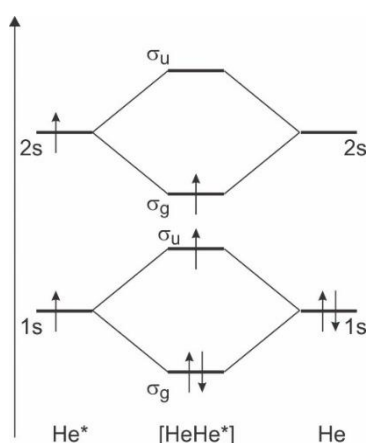
For O₂ LUMO as for C₂²⁻, HOMO:



- 2.30** 15.2 eV corresponds to excitation of the electrons from 3σ MO in CO. Peaks between 17 and about 17.8 eV correspond to the excitation of 1π electrons, and the peak highest in energy corresponds to the excitation of 2σ electrons.

The UV PES for SO should have one more line at even lower energies corresponding to the ionization from 2π degenerate set of molecular orbitals.

2.31



Bond order is 1.

- 2.32** N_2 MO diagram see Figure 2.18, O_2 MO diagram see Figure 2.12 and NO see Figure 2.22 (for CO). The bond order for NO is 2.5 and is in between that for N_2 (3) and O_2 (2), hence bond length in NO is in the middle.

- 2.33** a) Square H_4^{2+} not likely to exist, no duplet of electrons.
b) Each O has an octet, likely to exist.

Chapter 3

Self-Tests

- 3.1** Three S_4 axes.
3.2 a) BF_3 D_{3h}
b) SO_4^{2-} T_d .

- 3.3** d_{z^2} and $d_{x^2-y^2}$ are A_1 , d_{xy} is A_2 , d_{yz} is B_2 and d_{xz} is B_1 .

- 3.4** Three.

- 3.5** Point group is D_{5d} , not polar.

- 3.6** It is chiral, but optical isomers very unlikely to be observed under normal conditions.

- 3.7** It is Raman active as well.

- 3.8** The first row in the D_{2h} character table, which is the A_g symmetry type.

- 3.9** $A_{1g} + B_{1g}$ are Raman active, E_u is IR active.

- 3.10** A_1

- 3.11** B_{1g}

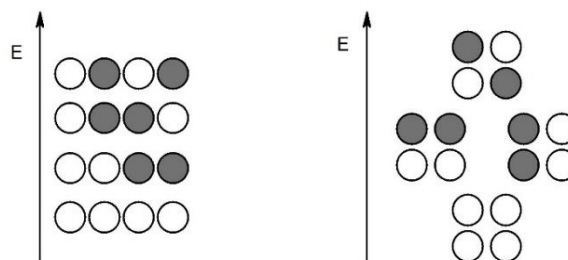
- 3.12** $5s$ and $4d_{z^2}$ have A_{1g} symmetry; $d_{x^2-y^2}$ has B_{1g} symmetry; and $5p_x$ and $5p_y$ have E_u symmetry.

- 3.13** For *trans*- SF_4Cl_2 we will observe two IR and three Raman stretching absorptions, whereas for SF_6 only one IR and two Raman absorptions.

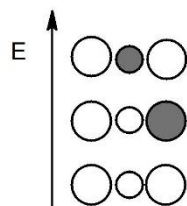
- 3.14** $A_{1g} + B_{1g} + B_{2g} + A_{2u} + B_{2u} + 2E_u$.

- 3.15** $A_{1g} + E_g + T_{1u}$.

- 3.16** For linear H_4 is on the left; for square on the right. Square H_4 is paramagnetic.

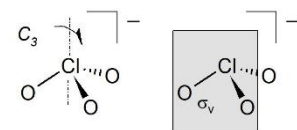
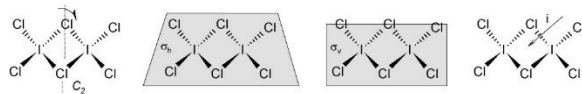
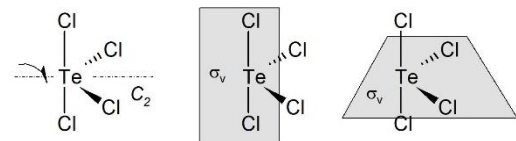
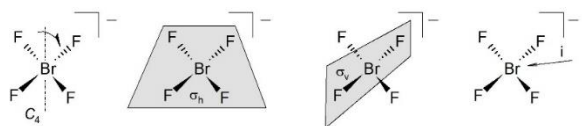


3.17

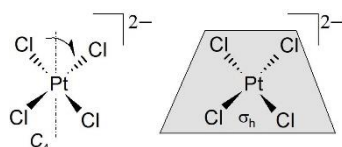
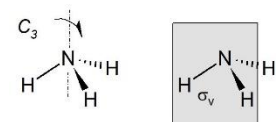


Exercises

3.1



3.2



- 3.3** a) CO_2 : i , and S_4 .
b) C_2H_2 : i and S_4 .

- c) BF_3 : neither i nor S_4 .
d) SO_4^{2-} : three S_4 axes, coincident with three C_2 axes, no i .

- 3.4** a) NH_2Cl ? C_s
b) CO_3^{2-} ? D_{3h}
c) SiF_4 ? T_d
d) HCN ? $C_{\infty v}$.
e) SiFCIBrI ? C_1 .
f) BrF_4^- ? D_{4h} .

- 3.5** C_6H_6 has even mirror planes, 1,3,5-trichlorobenzene has four.

- 3.6** a) possess an infinite number of mirror planes that pass through both lobes and include the long axis of the orbital. In addition, the long axis is a C_n axis, where n can be any number from 1 to ∞ .
b) Center of inversion and three mutually perpendicular C_2 axes, each one coincident with one of the three Cartesian coordinate axes. Furthermore, it possesses three mutually perpendicular mirror planes of symmetry, which are coincident with the xy plane and the two planes that are rotated by 45° about the z -axis from the xz plane and the yz plane.
c) In addition to the symmetry elements possessed by a p orbital, also (i) a centre of symmetry, (ii) a mirror plane that is perpendicular to the C_∞ axis, (iii) an infinite number of C_2 axes that pass through the centre of the orbital and are perpendicular to the C_∞ axis, and (iv) an S_∞ axis.

- 3.7** a) C_{3v}
b) 2
c) $3p_x$ and $3p_y$.

- 3.8** a) D_{3h}
b) 2
c) $3p_x$ and $3p_y$.

- 3.9** 12 vibrational modes, six Raman bands: $2A_1' + 3E' + E''$.

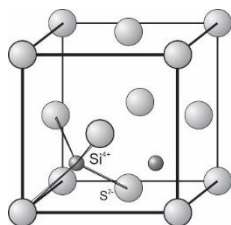
- 3.10** a) 5
b) 1
- 3.11** a) None
b) The E' modes are active in both IR and Raman.
- 3.12** $s = (1/2)(\varphi_1 + \varphi_2 + \varphi_3 + \varphi_3) (= A_1)$
 $p_x = (1/2)(\varphi_1 - \varphi_2 + \varphi_3 - \varphi_3) (= T_2)$
 $p_y = (1/2)(\varphi_1 - \varphi_2 - \varphi_3 + \varphi_3) (= T_2)$
 $p_z = (1/2)(\varphi_1 + \varphi_2 - \varphi_3 - \varphi_3) (= T_2)$
- 3.13** a) BF_3
 $(1/\sqrt{3})(\varphi_1 + \varphi_2 + \varphi_3) (= A_1')$
 $(1/\sqrt{6})(2\varphi_1 - \varphi_2 - \varphi_3)$ and $(1/\sqrt{2})(\varphi_2 - \varphi_3)$
 $(= E')$
 b) PF_5 (axial F atoms are $\varphi_4 + \varphi_5$)
 $(1/\sqrt{2})(\varphi_4 + \varphi_5) (= A_1')$
 $(1/\sqrt{2})(\varphi_4 - \varphi_5) (= A_2'')$
 $(1/\sqrt{3})(\varphi_1 + \varphi_2 + \varphi_3) (= A_1')$
 $(1/\sqrt{6})(2\varphi_1 - \varphi_2 - \varphi_3)$ and $(1/\sqrt{2})(\varphi_2 - \varphi_3) (= E')$
- 3.14** See Figure 3.30 for MO diagram. the electron configuration $1a_1^2 1e^4 2a_1^2$ results in only three bonds $((2 + 4)/2 = 3)$. Since there are three N–H bonds, the average N–H bond order is 1 $(3/3 = 1)$.
- 3.15** HOMO (e set) pure F atom SALC; LUMO ($2t_1$ set) both S and F character with more S.

Chapter 4

Self-Tests

- 4.1** P-type lattice of chloride anions with caesium cations in cubic hole.

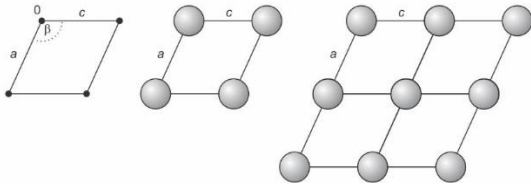
4.2



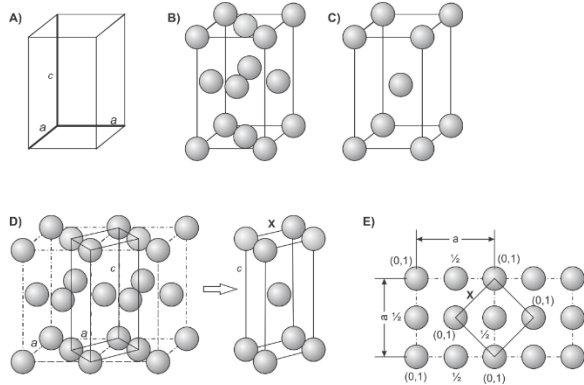
- 4.3** a) 52%
b) 68%
- 4.4** $r_{\text{hole}} = ((3/2)^{1/2} - 1)r = 0.225r$.
- 4.5** The spheres-to-tetrahedral holes ratio in this cell is 4 : 8 or 1 : 2.
- 4.6** 409 pm.
- 4.7** 401 pm.
- 4.8** FeCr_3 .
- 4.9** X_2A_3 .
- 4.10** a) PrO_2 likely fluorite-type.
b) CrO_2 likely rutile-type
 c) CrTaO_4 likely rutile-type
 d) AcOF likely fluorite-type
 e) Li_2TiF_6 likely antifluorite-type.
- 4.11** The coordination of O^{2-} is two Ti^{4+} and four Ca^{2+} and longer distances.
- 4.12** LaImO_3 .
- 4.13** CaO : NaCl structure; BkO_2 : TiO_2 structure.
- 4.14** 2421 kJ mol^{-1} .
- 4.15** Unlikely to exist.
- 4.16** 2602 kJ mol^{-1} .
- 4.17** $\text{MgSO}_4 < \text{CaSO}_4 < \text{SrSO}_4 < \text{BaSO}_4$.
- 4.19** a) Frenkel defects.
b) Schottky defects.
- 4.20** Phosphorus and aluminium.
- 4.21** The $d_{x^2-y^2}$ and d_{z^2} have lobes pointing along the cell edges to the nearest neighbour metals.
- 4.22** V_2O_5 n -type; CoO p -type.

Exercises

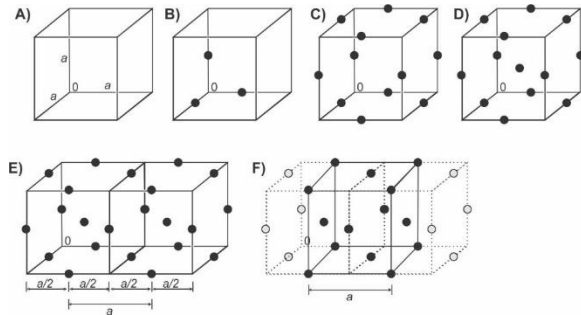
4.1 $a \neq b \neq c$ and $\alpha = 90^\circ, \beta \neq 90^\circ, \gamma = 90^\circ$



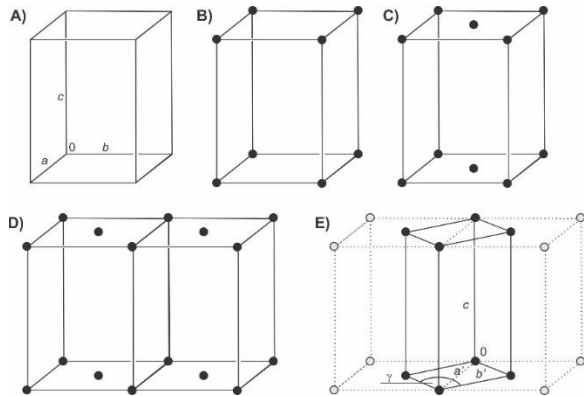
4.2



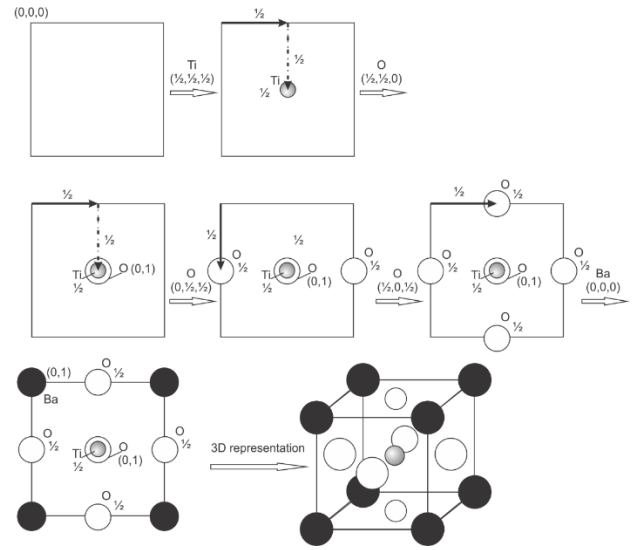
4.3 a) Face-centered, four lattice points



b) Tetragonal primitive, one lattice point



4.4 Perovskite-type structure



4.5 Scheme c).

4.6 MX_2 , MX_2 and MX_3 .

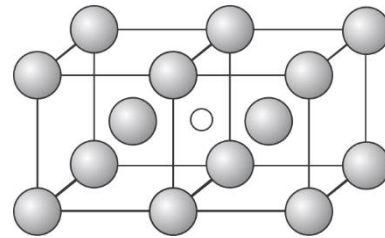
4.7 See Figure 4.5 in the textbook for the unit cell, $a = 361 \text{ pm}$ and $r(\text{Cu}) = 128 \text{ pm}$.

4.8 K_3C_{60}

4.9



4.10 The shortest distance is 254 pm.



4.11 $a = 351 \text{ pm}$.

4.12 12 carat.

4.13 An alloy.

4.14 a) LiI ionic
b) BeBr₂ ionic

- c) SnS covalent
d) RbSn Zintl phase.
- 4.15** a) In NaCl coordination is (6, 6) in CsCl is (8, 8)
b) In CsCl.
- 4.16** Cs⁺ has six second nearest neighbours, and 24 third-nearest neighbours.
- 4.17** Re coordination is six, oxygen is two; the perovskite-type structure is generated.
- 4.18** M(OH)₃, M could be La³⁺ and In³⁺.
- 4.19** A has coordination number 12, B coordination number 6.
- 4.20** a) MX₂ b) M₂X c) M₂X₃; coordination numbers in a) for M is six for X is three, in b) for M is four and for X is eight.
- 4.21** One quarter.
- 4.22** a) UO₂: TiO₂ type
b) FrI: CsCl type
c) BeS: ZnS type
d) InN: NaCl or NiAs type.
- 4.23** Mg²⁺ 79.8 pm, Ca²⁺ 102.8 pm, and Ba²⁺ = 138.3 pm.
- 4.24** a) LiF (6,6)
b) RbBr (6,6)
c) SrS (6,6)
d) BeO (6,6): Be²⁺ with its small size and relatively high charge and electronegativity forms compounds with significant covalent character resulting in higher directionality of chemical bonds
- 4.25** The complex ions ([PtCl₆]²⁻, [Ni(H₂O)₆]²⁺, [SiF₆]²⁻, PF₆⁻) are symmetric and their shape can be approximated with a sphere. For (a) we predict an antifluorite structure, for (b) a CsCl structure type., for (c) CN⁻ is a similar sized anion compared to Cs⁺ cationic radius of ~180

pm we predict a CsCl structure type, for (d) NaCl structure type.

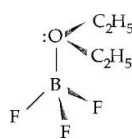
- 4.26** Calcite's rhombohedral unit cell can be obtained if we take cubic NaCl unit cell and pull its opposite corners across the body diagonal apart.
- 4.27** The figure shows wurtzite structure type. The A_pB_{2q} structure can be derived by removing every second A from the structure of AB.
- 4.28** The lattice enthalpy for Ca₃N₂ and bond dissociation energy for N₂.
- 4.29** we can expect significant energy demand for the Ag(g) ionization step (*I*₁ + *I*₂) for both compounds. The bond dissociation energy (*BDE*) for Cl₂ is higher than that for F₂ adding in energy requirement for AgCl₂. The electron affinity, a process that releases energy, is more negative for F(g) than for Cl(g). Also, it is expected that AgF₂ lattice enthalpy will be much higher than that of AgCl₂ on the account of smaller F⁻ size as Δ*H*^o_L is proportional to 1/*d*.
- 4.30** CsI < RbCl < LiF < SrO < NiO < AlP.
- 4.31** For MgO the lattice enthalpy is about four times while for AlN nine times the NaCl value.
- 4.32** Lattice enthalpy 1990 kJ mol⁻¹; *I*₂ for K is very high.
- 4.33** Lattice enthalpy is 717 kJ mol⁻¹, from the Born-Haber cycle the enthalpy of formation for CaCl is -185 kJ mol⁻¹, higher lattice enthalpy for CaCl₂ and gain of *I*₁ for Ca make disproportionation favourable reaction.
- 4.34**
$$\frac{e^2}{\pi\epsilon_0 a} \left(-\frac{4}{\sqrt{3}} + \frac{3}{2} + \frac{3}{\sqrt{2}} - \frac{12}{\sqrt{11}} \right)$$
- 4.35** AgCl has a significant covalent character, while the equation is based on pure ionic bonding; discrepancy could be expected for Ca²⁺ and Hg²⁺ (CaCl₂ vs. HgCl₂).

- 4.36 a) BkO_2 10906 kJ mol^{-1}
 b) K_2SiF_6 1888 kJ mol^{-1}
 c) LiClO_4 664 kJ mol^{-1} .
- 4.37 a) CaSeO_4 , b) NaBF_4
- 4.38 CsI has the lowest lattice enthalpy and highest solubility.
- 4.39 Ba^{2+} is a good candidate for SeO_4^{2-} ; Na^+ would give a soluble phosphate, Ba^{2+} an insoluble phosphate.
- 4.40 a) MgCO_3 b) CsI_3
- 4.41 Cs^+ or a tetraalkylammonium cation, such as tetraethylammonium, $(\text{CH}_3\text{CH}_2)_4\text{N}^+$.
- 4.42 a) Schottky b) Frenkel
- 4.43 Fe^{2+} and Ti^{4+} substituting for Al^{3+} .
- 4.44 Vanadium carbide and manganese sulfide.
- 4.45 The term $-T\Delta S$ becomes more negative as defects are formed because they introduce more disorder into the lattice and the entropy rises; increase in the pressure also reduces the spacing between the ions in the structure increasing the energy associated with ion removal and displacement within the structure, thereby increasing the free energy of defect formation.
- 4.46 Fe_{1-x} and UO_{2+x} .
- 4.47 a) *p*-type
 b) *n*-type
 c) *n*-type
- 4.48 VO
- 4.49 A semiconductor is a substance with an electrical conductivity that decreases with increasing temperature. It has a small, measurable band gap. A semimetal is a solid whose band structure has a zero density of states and no measurable band gap.
- 4.50 Ag_2S and CuBr *p*-type; VO_2 *n*-type.

- 4.51 In KC_8 potassium donates the electrons to the upper band which was originally empty in the graphite structure. In C_8Br bromine removes some electrons from the filled lower band in the graphite structure. In either case the net result is a partially filled band (formed either by addition of electrons to the originally empty band or by removal of electrons from the initially filled band) and both KC_8 and C_8Br should have metallic properties.

Chapter 5

Self-tests

- 5.1 a) HNO_3 acid, H_2O base; NO_3^- conjugate base, H_3O^+ conjugate acid
 b) CO_3^{2-} base, H_2O acid; HCO_3^- conjugate acid, OH^- conjugate base
 c) NH_3 base, H_2S acid; NH_4^+ conjugate acid, HS^- conjugate base.
- 5.2 pH = 2.24
- 5.3 pH = 1.85
- 5.4 $[\text{Na}(\text{H}_2\text{O})_6]^+$ (least acidic) < $[\text{Mn}(\text{H}_2\text{O})_6]^{2+}$ < $[\text{Ni}(\text{H}_2\text{O})_6]^{2+}$ < $[\text{Sc}(\text{H}_2\text{O})_6]^{3+}$.
- 5.5 a) 3 b) 8 c) 13
- 5.6 TiO_2 is amphoteric: addition of base would first precipitate TiO_2 which would be re-dissolved in excess of base; no reaction with H_2O_2 .
- 5.7 a) FeCl_3 acid, Cl^- base
 b) I^- base, I_2 acid.
- 5.8 $(\text{H}_3\text{Si})_3\text{N}$ is planar, $(\text{H}_3\text{C})_3\text{N}$ is pyramidal.
- 5.9 DMSO and NH_3
- 5.10 Base.
- 5.11 

Exercises

5.1

1	1											
1	1											
1	1											
2	3	4						6	7	8	9	10
2	3	4	5	6	7	8	9	10	11	12	13	
2	3	4	5	6	7	8	9	10	11	12	13	
2	3	4	5	6	7	8	9	10	11	12	13	
3	11	12						14	15	16	17	
3	11	12	13	14	15	16	17	18	19	20	21	
3	11	12	13	14	15	16	17	18	19	20	21	
4	19	20						22	23	24	25	
4	19	20	21	22	23	24	25	26	27	28	29	
4	19	20	21	22	23	24	25	26	27	28	29	
5	37	38						40	41	42	43	
5	37	38	39	40	41	42	43	44	45	46	47	
5	37	38	39	40	41	42	43	44	45	46	47	
6	55	56						58	59	60	61	
6	55	56	57	58	59	60	61	62	63	64	65	
6	55	56	57	58	59	60	61	62	63	64	65	
7	87	88						90	91	92	93	
7	87	88	89	90	91	92	93	94	95	96	97	
7	87	88	89	90	91	92	93	94	95	96	97	

5.2 $[\text{Co}(\text{NH}_3)_5(\text{OH})]^{2+}$, SO_4^{2-} , CH_3O^- , H_2PO_4^- , $\text{SiO}(\text{OH})_3^-$ and S^{2-} .

5.3 $\text{C}_5\text{H}_5\text{NH}^+$ (pyridinium), H_2PO_4^- , HO^- , $\text{CH}_3\text{C}(\text{OH})_2^+$, $[\text{HCo}(\text{CO})_4]$, HCN .

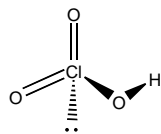
5.4 $[\text{H}_3\text{O}^+] = 1.4 \times 10^{-3}$, $\text{pH} = 2.85$

5.5 5.6×10^{-10} .

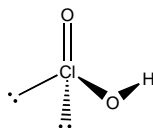
5.6 5.6×10^{-6} .

5.7 As a base.

5.8 For chloric -2 , for chlorous 3 .



chloric acid



chlorous acid

5.9 i) CO_3^{2-} measurable, O^{2-} too strong, NO_3^- and ClO_4^- too weak.

ii) HSO_4^- and NO_3^- are measurable, ClO_4^- too weak

5.10 Electron withdrawing.

5.11 The difference in $\text{p}K_a$ values can be explained by looking at the structures of the acids.

5.12 Na^+ (weakest) $< \text{Sr}^{2+} < \text{Ca}^{2+} < \text{Mn}^{2+} < \text{Fe}^{3+} < \text{Al}^{3+}$.

5.13 $\text{HClO}_4 (-7) > \text{HBrO}_3 (-2) > \text{H}_2\text{SO}_4 (-2) > \text{HNO}_2 (3)$.

5.14 a) $[\text{Fe}(\text{H}_2\text{O})_6]^{3+}$

b) $[\text{Al}(\text{H}_2\text{O})_6]^{3+}$

c) $\text{Si}(\text{OH})_4$

d) HClO_4

e) HMnO_4

f) H_2SO_4

5.15 $\text{Cl}_2\text{O}_7 < \text{SO}_3 < \text{CO}_2 < \text{B}_2\text{O}_3 < \text{Al}_2\text{O}_3 < \text{BaO}$.

5.16 $\text{NH}_3 < \text{CH}_3\text{GeH}_3 < \text{H}_4\text{SiO}_4 < \text{HSO}_4^- < \text{H}_3\text{O}^+ < \text{HSO}_3\text{F}$.

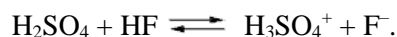
5.17 Ag^+ is a stronger acid, due to difference in bonding.

5.18 Reduction in charge for one unit per M.

5.19 a) $\text{H}_3\text{PO}_4(\text{aq}) + \text{HPO}_4^{2-}(\text{aq}) \rightleftharpoons 2\text{H}_2\text{PO}_4^-(\text{aq})$

b) $\text{CO}_2(\text{aq}) + \text{CaCO}_3(\text{s}) + \text{H}_2\text{O}(\text{l}) \rightleftharpoons \text{Ca}^{2+}(\text{aq}) + 2\text{HCO}_3^-$.

5.20 Acid:



Base:



5.21 H–Se bond is weaker than H–S bond.

5.22 There is no p-p π interaction in Si halides and their Lewis acidity is dictated only by the electronegativity difference.

5.23 a) The acids in this reaction are the Lewis acids SO_3 and H^+ and the base is the Lewis base OH^- . This is a displacement reaction.

b) This is a displacement reaction. The Lewis acid Hg^{2+} displaces the Lewis acid $[\text{B}_{12}]$ from the Lewis base CH_3^- .

c) This is also a displacement reaction. The Lewis acid SnCl_2 displaces the Lewis acid K^+ from the Lewis base Cl^- .

d) It is a displacement reaction. The very strong Lewis acid SbF_5 (one of the strongest known) displaces the Lewis acid $[\text{AsF}_2]^+$ from the Lewis base F^- .

e) A Lewis acid–base complex formation reaction between EtOH (the acid) and py (the base) produces the adduct EtOH-py , which is held together by a hydrogen bond.

5.24 a) 1st row BBr_3 ; 2nd row BCl_3 ; 3rd row $\text{B}(\text{nBu})_3$

b) 1st row Me_3N ; 2nd row 4- $\text{CH}_3\text{C}_5\text{H}_4\text{N}$.

5.25 a) < 1 b) > 1 c) < 1 d) > 1.

5.26 a) CsBrF_4 , F^- Lewis base, BrF_3 Lewis acid.

b) $[\text{ClF}_2][\text{SbF}_6]$, F^- Lewis base, SbF_5 Lewis acid

c) $[\text{B}(\text{OH})_3(\text{H}_2\text{O})]$, H_2O Lewis base, $\text{B}(\text{OH})_3$ Lewis acid

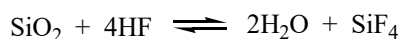
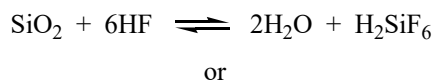
d) $[\text{BH}_3(\text{PMe}_3)]$, PMe_3 Lewis base, B_2H_6 Lewis acid.

5.27 Three methyl groups on N atom increase the steric demands.

5.28 a) DMSO is a stronger base always, but the ambiguity arises because DMSO has two Lewis basic centres: S atom and O atom.

b) Depends on E_A and C_A values of the acid.

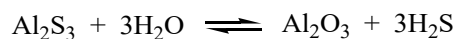
5.29



The Brønsted reaction involves the transfer of protons from HF molecules to O^{2-} ions, whereas the Lewis reaction

involves complex formation between $\text{Si}(\text{IV})$ centre and F^- ions.

5.30 An equilibrium is established between two hard acids, $\text{Al}(\text{III})$ and H^+ , and the bases O^{2-} and S^{2-} :



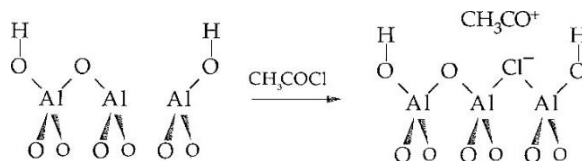
5.31 a) solvent should be hard and acidic (i.e., HF)

b) hard acid (in this case alcohols)

c) hard base (such as ether)

d) Softer base than Cl^- (i.e., CH_3CN).

5.32



5.33 Hg^{2+} is a soft Lewis acid and prefers soft Lewis base S^{2-} ; Zn^{2+} is a borderline Lewis acid.

5.34 a) $\text{CH}_3\text{CH}_2\text{OH} + \text{HF} \rightleftharpoons \text{CH}_3\text{CH}_2\text{OH}_2^+ + \text{F}^-$

b) $\text{NH}_3 + \text{HF} \rightleftharpoons \text{NH}_4^+ + \text{F}^-$

c) $\text{C}_6\text{H}_5\text{COOH} + \text{HF} \rightleftharpoons \text{C}_6\text{H}_5\text{COO}^- + \text{H}_2\text{F}^+$.

5.35 The dissolution of silicates in HF is both a Brønsted acid–base reaction and a Lewis acid–base reaction.

5.36 They are hard acids.

5.37 $-20.0 \text{ kJ mol}^{-1}$.

5.38 The lowest solvation energy is going to be observed for the largest cation of the group.

5.39 $\text{CO}_2(\text{g}) \rightleftharpoons \text{CO}_2(\text{aq})$ (1)

$\text{CO}_2(\text{aq}) + \text{H}_2\text{O}(\text{l}) \rightleftharpoons \text{H}_2\text{CO}_3(\text{aq})$ (2)

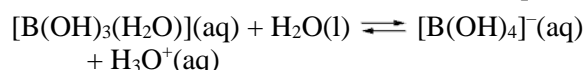
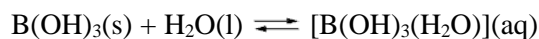
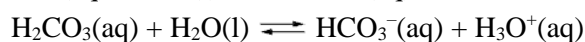
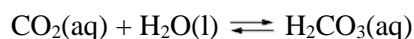
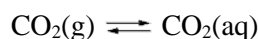
$\text{M}_2\text{SiO}_4(\text{s}) + 4\text{H}_2\text{CO}_3(\text{aq}) \rightleftharpoons 2\text{M}^{2+} + \text{Si}(\text{OH})_4(\text{aq}) + 4\text{HCO}_3^-(\text{aq})$ (3)

- 5.40** a) $\text{Fe}^{3+}(\text{aq}) + 6\text{H}_2\text{O}(\text{l}) \rightleftharpoons \text{Fe}(\text{OH})_3(\text{s}) + 3\text{H}_3\text{O}^+$
 b) 0.1547 M; pH= 1.6; neglected Fe^{3+} containing species are $\text{Fe}(\text{OH})_2^+$ and $\text{Fe}(\text{OH})^{2+}$.
- 5.41** With increasing charge density the attraction between M^{2+} cation and partially negative O atom in H_2O is increasing. For the same reason, the acidity of these aqua acids is increasing showing that two trends correlate closely.
- 5.42** $[\text{AlCl}_2(\text{NCCH}_3)_4]^+$ and $\text{Cl}^-(\text{sol})$.
- 5.43** Equation (b) is better in explaining the observations described in the exercise.
- 5.44** this borderline does agree with describing S^{2-} as a softer base than O^{2-} .
- 5.45** *S is the radioactively labelled sulfur atom:
- $$*\text{SO}_2 + \text{Cl}^- \rightleftharpoons *\text{SO}_2\text{Cl}^-$$
- $$*\text{SO}_2\text{Cl}^- + \text{SOCl}_2 \rightleftharpoons *\text{SOCl}_2 + \text{SO}_2\text{Cl}^-$$
- $$\text{SO}_2\text{Cl}^- \rightleftharpoons \text{SO}_2 + \text{Cl}^-$$
- $$*\text{SOCl}_2 + \text{SbCl}_5 \rightleftharpoons *\text{SOCl}_2 \cdot \text{SbCl}_5$$
- $$*\text{SOCl}_2 \cdot \text{SbCl}_5 \rightleftharpoons \text{SOCl}_2 \cdot \text{SbCl}_5 + *\text{SO}_2$$
- $$\text{SOCl}_2 \cdot \text{SbCl}_5 \rightleftharpoons \text{SOCl}_2 + \text{SbCl}_5.$$
- 5.46** The reasons for the difference in stability are steric.
- 5.47** a) < 1 b) > 1 c) > 1
- 5.48** a) $\text{Fe}(\text{ClO}_4)_3$
 b) $\text{Mg}(\text{NO}_3)_2$
 c) $\text{Zn}(\text{NO}_3)_2$.
- 5.49** Cations such as I_2^+ and Se_8^{2+} should behave like good Lewis acids while anions such as S_4^{2-} and Pb_9^{4-} are good Lewis bases.
- 5.50** For titration of a weak base with a strong acid we have to find a solvent other than water in which a weak base is going to

behave as strong one and give us a sharp and easy to detect end point. To achieve this, we have to find solvent more acidic than water, which can be acetic acid.

- 5.51** a) The p-p π interaction in $\text{B}(\text{OMe})_3$ lowers the acidity of this compound.
 b) Delocalization of N's lone electron pair lowers the basicity of $\text{N}(\text{SiH}_3)_3$.

5.52

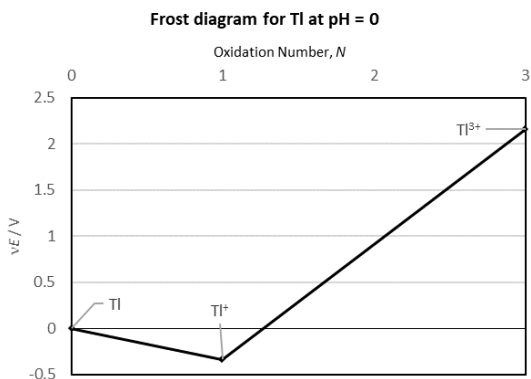


Chapter 6

Self-tests

- 6.1** $2\text{MnO}_4^-(\text{aq}) + 5\text{Zn}(\text{s}) + 16\text{H}^+(\text{aq}) \rightarrow 5\text{Zn}^{2+}(\text{aq}) + 2\text{Mn}^{2+}(\text{aq}) + 8\text{H}_2\text{O}(\text{l})$.
- 6.2** No.
- 6.3** Yes; the side reaction with Cl^- should be expected.
- 6.4** +1.25 V.
- 6.5** It is converted to sulfate, SO_4^{2-} .
- 6.6** No.
- 6.7** Bpy prefers Ru(II). For 17 orders of magnitude relative to water.
- 6.8** +0.223 V.
- 6.9** a) Yes b) No.

6.10



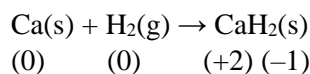
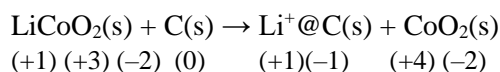
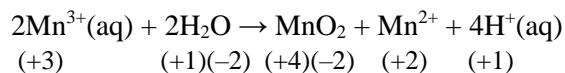
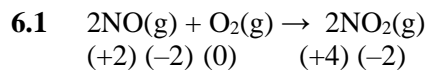
6.11 +2.

6.12 NO₃⁻ is a stronger oxidizing agent in an acidic medium than in basic.

6.13 Fe²⁺(aq) is a predominant species; Fe(OH)₃ is unstable.

6.14 2000°C or above.

Exercises



6.2 a) For example S₂O₈²⁻, H₂O₂, a-PbO₂ or MnO₄⁻

b) For example, Mn, Zn or NH₃OH

c) For example, Cu

d) For example, H₂S.

6.3 a) $4\text{Cr}^{2+}(\text{aq}) + \text{O}_2(\text{g}) + 4\text{H}^+(\text{aq}) \rightarrow 4\text{Cr}^{3+}(\text{aq}) + 2\text{H}_2\text{O}(\text{l}), E^\circ = +1.65 \text{ V}$

b) $4\text{Fe}^{2+}(\text{aq}) + \text{O}_2(\text{g}) + 4\text{H}^+(\text{aq}) \rightarrow 4\text{Fe}^{3+}(\text{aq}) + 2\text{H}_2\text{O}(\text{l}), E^\circ = +0.46 \text{ V}$

c) No reaction

d) No reaction

e) $2\text{Zn}(\text{s}) + \text{O}_2(\text{g}) + 4\text{H}^+(\text{aq}) \rightarrow 2\text{Zn}^{2+}(\text{aq}) + 2\text{H}_2\text{O}(\text{l}), E^\circ = +1.99 \text{ V}$ with a competing reaction:

$\text{Zn}(\text{s}) + 2\text{H}^+(\text{aq}) \rightarrow \text{Zn}^{2+}(\text{aq}) + \text{H}_2(\text{g}) (E^\circ = +0.763 \text{ V}).$

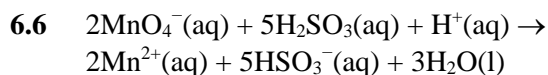
6.4 a) (i) Fe³⁺ will not oxidize water, (ii) Fe²⁺ will not reduce water, (iii) Fe²⁺ will be oxidized to Fe³⁺ by O₂, (iv) disproportionation will not occur

b) Ru²⁺ will not oxidize or reduce water, O₂ would oxidize Ru²⁺ to Ru³⁺, Ru²⁺ will disproportionate to Ru³⁺ and Ru

c) HClO₂ will oxidize water (not reduce it), O₂ will oxidize HClO₂ to HClO₃, HClO₂ will disproportionate to ClO₃⁻ and HClO

d) Br₂ will not oxidize or reduce water, will not be oxidized by O₂ and will not disproportionate to Br⁻ and HBrO.

6.5 The change in temperature has the opposite effect on one or both K values for the two complexes.



The potential decreases as the pH increases.

6.7

Redox couple	Ti ³⁺ /Ti ²⁺	V ³⁺ /V ²⁺	Cr ³⁺ /Cr ²⁺	Mn ³⁺ /Mn ²⁺	Fe ³⁺ /Fe ²⁺	Co ³⁺ /Co ²⁺
E°	+0.67	+0.77	+1.18	+0.92	-0.29	-1.26

6.8 a) $E = E^\circ - \frac{0.059 \text{ V}}{4} \left(\log \frac{1}{p(\text{O}_2)} + 4\text{pH} \right).$

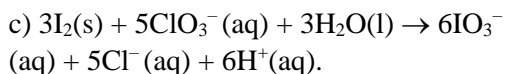
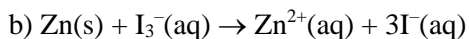
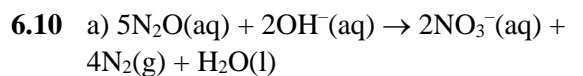
b) $E = E^\circ - 0.059 \text{ V} \times \text{pH}$

At pH = 7 and O₂ pressure 0.20 the potential is +0.81 V.

6.9 a) Cl₂ disproportionates to Cl⁻ and ClO₄⁻.

b) Cl_2 can (thermodynamically) oxidize water.

c) Kinetic.



6.11 $E = -0.21 \text{ V}$.

6.12 a) basic

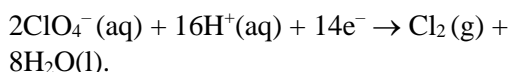
b) acidic

c) basic

b) No difference.

6.13 It is thermodynamically favourable for OH_2 to disproportionate.

6.14 $E = +1.39 \text{ V}$



6.15 $E = +0.387 \text{ V}$.

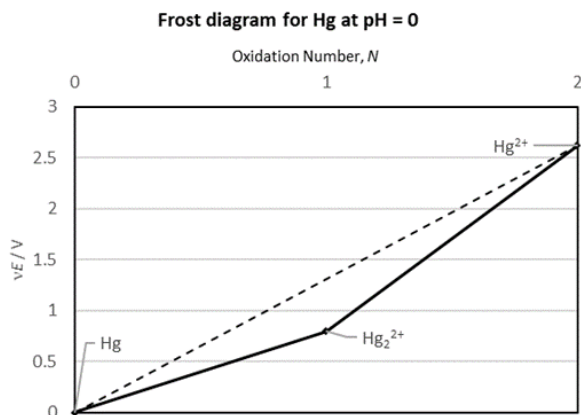
6.16 $E = +0.98 \text{ V}$.

6.17 $K = 4.37 \times 10^{10}$.

6.18 $K = 5.7 \times 10^{38}$.

6.19 The reduction potential become less positive.

6.20



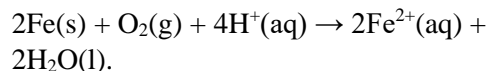
Hg^{2+} is a potentially good oxidizing agent; Hg and Hg^{2+} are going to comproportionate to give Hg_2^{2+} .

6.21 a) $\text{Fe}(\text{OH})_3$ precipitate

b) solid Mn_2O_3

c) HSO_4^- .

6.22 The corrosion of iron:



Dissolved CO_2 decreases the pH, open container increases O_2 concentration; both factors enable the corrosion.

6.23 Approximately -0.1 V .

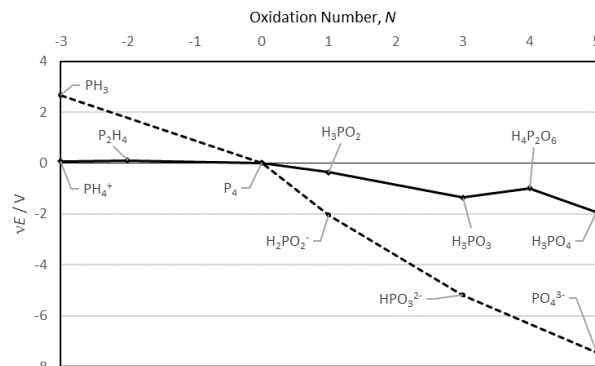
6.24 Any boundary between a soluble species and an insoluble species will change as the concentration of the soluble species changes. The boundaries between the two soluble species, and between the two insoluble species, will not depend on the choice of $[\text{Fe}^{2+}]$.

6.25 Above 1600°C

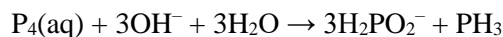
6.26 a) The reduction process depends on the concentration of H^+ .

b)

Frost diagram for P at pH = 0 (solid line) and pH = 14 (dashed line)



c) Reaction



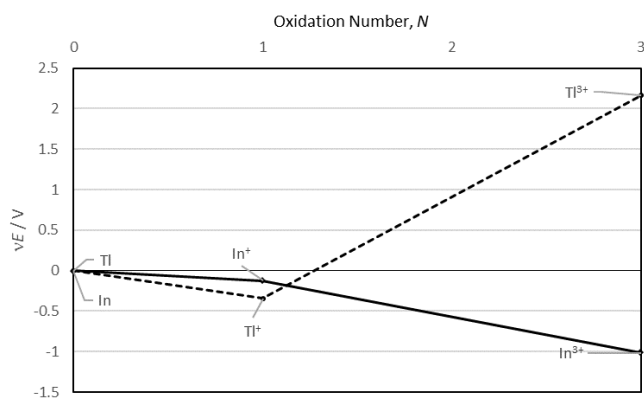
Has equilibrium constant $K = 7.1 \times 10^{58}$.

- 6.27** a) 0.716 V , $-207.2 \text{ kJ mol}^{-1}$, 2.1×10^{36}
 b) 0.726 V , $-70.0 \text{ kJ mol}^{-1}$, 1.9×10^{12}
 E and E° do not depend on the number of exchanged electrons, but K and the Gibbs energy do.

- 6.28** $\Delta_r H^\circ = 1386.1 \text{ kJ mol}^{-1}$
 $\Delta_r S^\circ = -0.282 \text{ kJ K}^{-1} \text{ mol}^{-1}$
 $\Delta_r G^\circ = 1302 \text{ kJ mol}^{-1}$
 $E^\circ = -2.25 \text{ V}$.

6.29

Frost diagram for In (solid line) and Tl (dashed line) at pH = 0

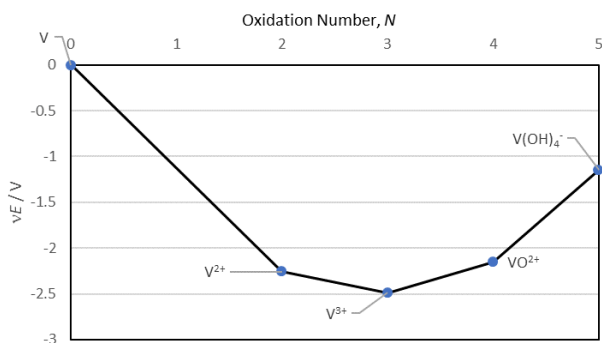


- 6.30** a) Ru^{2+} is less stable than Fe^{2+} in acidic aqueous solution
 b) $\text{Fe(s)} + 2\text{H}^+(\text{aq}) \rightarrow \text{Fe}^{2+}(\text{aq}) + \text{H}_2(\text{g})$
 c) $K = 3.7 \times 10^{62}$.

- 6.31** a) -2.28 V
 $\text{VO}^{2+} + 2\text{H}^+ + 4\text{e}^- \rightarrow \text{V} + \text{H}_2\text{O}$

b)

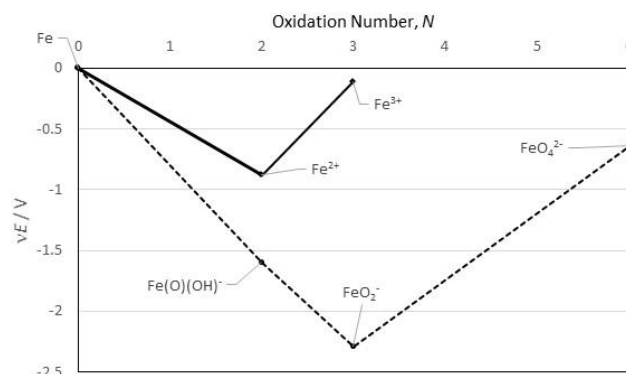
Frost diagram for V at pH = 0



- c) $K = 4.3 \times 10^{-24}$ (comproportionation reaction is more favourable than disproportionation)
 d) The potential becomes more negative with increase in pH.

6.32 a)

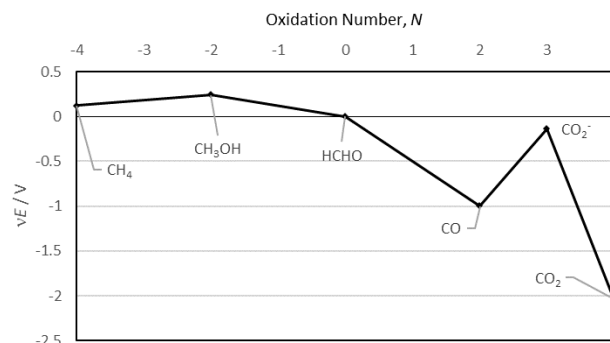
Frost diagram for Fe at pH = 0 (solid line) and pH = 14 (dashed line)



- b) $E^\circ = -0.04 \text{ V}$.
 c) Fe(III)/Fe(II) potentials involve different chemical species in acidic and basic solutions; FeO_4^{2-} can easily oxidize water under acidic conditions.
 d) $2\text{FeO}_2^- + 3\text{ClO}^- + 2\text{OH}^- \rightarrow 2\text{FeO}_4^{2-} + 3\text{Cl}^- + \text{H}_2\text{O}$.

- 6.33** a) CO_2 , +4; HCHO , 0; CO_2^- , +3; CO , +2; HCO_2^- , +2; CH_3OH , -2; and CH_4 , -4
 b)

Frost diagram for C at pH = 7



- d) Yes
 e) $K = 3.5 \times 10^{-32}$.

Chapter 7

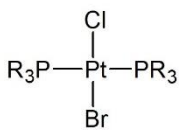
Self-Tests

- 7.1 a) $[\text{PtCl}_2(\text{OH}_2)_2]$
 b) $[\text{Cr}(\text{NCS})_4(\text{NH}_3)_2]^-$
 c) $[\text{Rh}(\text{en})_3]^{3+}$
 d) $[\text{MnBr}(\text{CO})_5]$
 e) $[\text{RhCl}(\text{PPh}_3)_3]$

- 7.2 The hydrate isomers
 $[\text{Cr}(\text{NO}_2)(\text{H}_2\text{O})_5]\text{NO}_2 \cdot \text{H}_2\text{O}$ and
 $[\text{Cr}(\text{H}_2\text{O})_6](\text{NO}_2)_2$; linkage isomer is
 $[\text{Cr}(\text{ONO})(\text{H}_2\text{O})_5]\text{NO}_2 \cdot \text{H}_2\text{O}$.

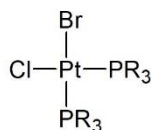
7.3

Complex A



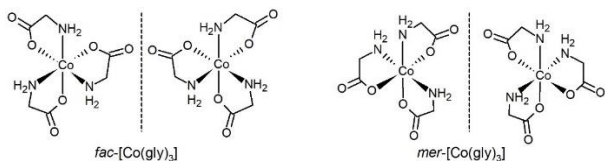
trans-[PtBrCl(PR₃)₂]

Complex B

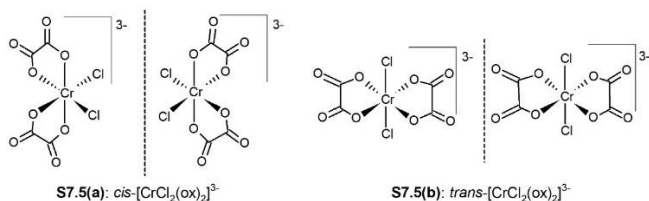


cis-[PtBrCl(PR₃)₂]

7.4



7.5

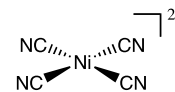


c) Achiral complex.

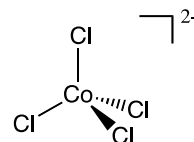
- 7.6 $K_{f1} = 1 \times 10^5$
 $K_{f2} = K_{f1} \times 5/6 = 1 \times 10^5 \times 5/6 = 0.83 \times 10^5$
 $K_{f3} = K_{f1} \times 4/6 = 1 \times 10^5 \times 4/6 = 0.67 \times 10^5$
 $K_{f4} = K_{f1} \times 3/6 = 1 \times 10^4 \times 3/6 = 0.50 \times 10^5$,
 $K_{f5} = K_{f1} \times 2/6 = 1 \times 10^5 \times 2/6 = 0.33 \times 10^5$, and
 $K_{f6} = K_{f1} \times 1/6 = 1 \times 10^5 \times 1/6 = 1.7 \times 10^5$.

Exercises

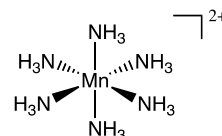
- 7.1 a) Tetracyanonickelate(II)



- b) Tetrachloridocobaltate(II)



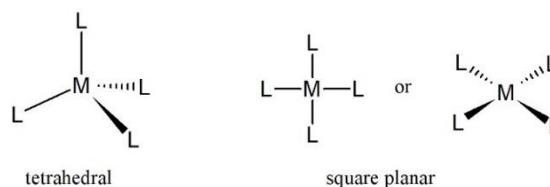
- c) Hexaamminemanganese(II)



- 7.2 a) $[\text{CoCl}(\text{NH}_3)_5]\text{Cl}_2$
 b) $[\text{Fe}(\text{OH}_2)_6](\text{NO}_3)_3$,
 c) *cis*-[RuCl₂(en)₂]
 d) $[\text{Cr}(\text{NH}_3)_5-\mu-\text{OH}-\text{Cr}(\text{NH}_3)_5]\text{Cl}_5$.

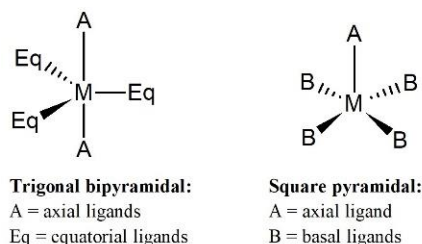
- 7.3 a) *cis*-tetraamminedichloridochromium(III)
 b) *trans*-diamminetetra(κ N-thiocyanato)-chromate(III)
 c) bis(1,2-diaminoethane)ethylenediamine-oxalatocobalt(III)

7.4 a)



b) Square planar.

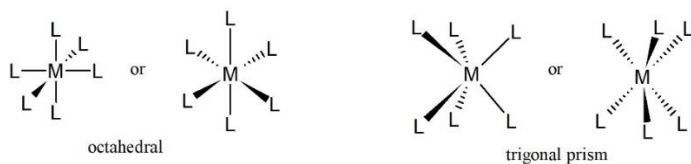
7.5



Trigonal bipyramidal:
 A = axial ligands
 Eq = equatorial ligands

Square pyramidal:
 A = axial ligand
 B = basal ligands

7.6 a)



b) Trigonal prism

7.7 A monodentate ligand can bond to a metal atom only at a single atom, also called a donor atom. A bidentate ligand can bond through two atoms, and a tetradentate ligand can bond through four atoms.

7.8 Linkage isomers: ligand examples are NO_2^- and SCN^- .

7.9 a) Bisdimethylphosphino ethane (dmpe): bidentate, chelating ligand that could also be a bridging ligand

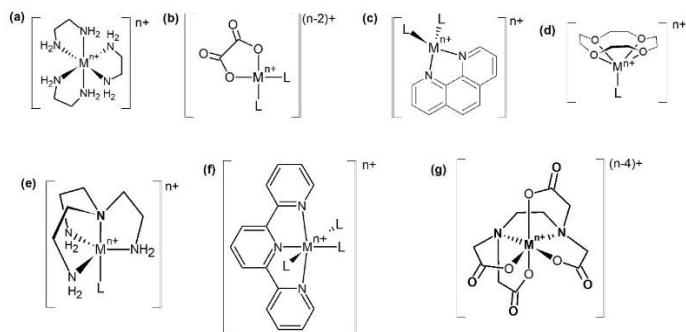
b) 2,2'-Bipyridine (bpy) is a bidentate, chelating ligand

c) Pyrazine is a monodentate ligand. The ligand can only bond to one metal; it can, however, bridge two metals.

d) Diethylenetriamine (dien) can be a tridentate ligand, can also act as a bidentate ligand and could be a bridging ligand.

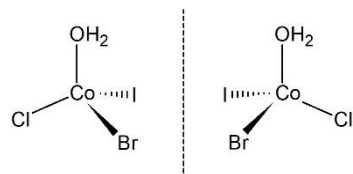
e) Tetraazacyclododecane ligand could be a tetradentate, macrocyclic ligand. This ligand could be bidentate and bridging.

7.10



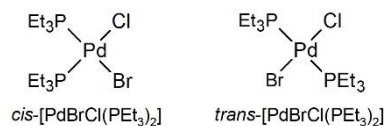
7.11 Ionization isomers

7.12 Only for $[\text{CoBrCl}(\text{OH}_2)]$.

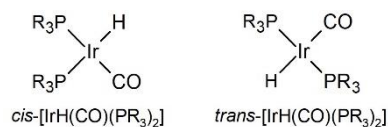


7.13 a) No isomers

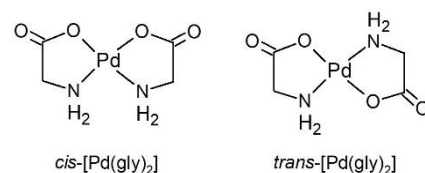
b) cis and trans:



c) cis and trans:

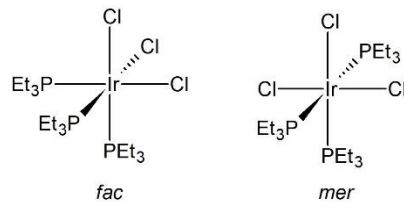


d) cis and trans:

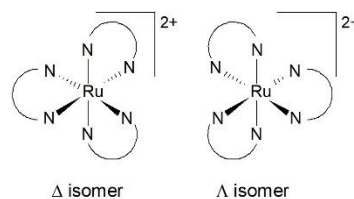


7.14 a) No isomers

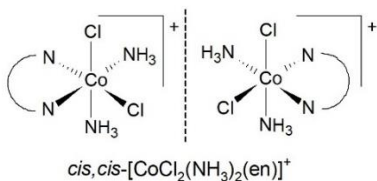
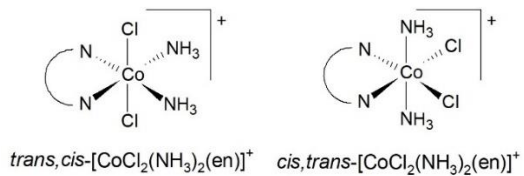
b) fac and mer:



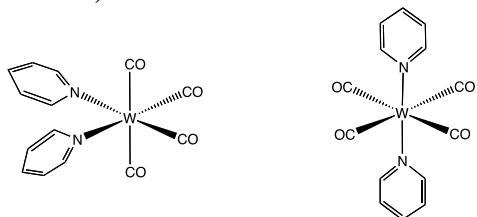
c) optical isomers:



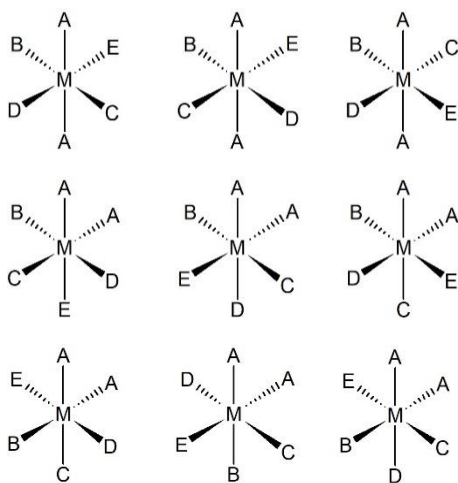
d) cis, trans and optical:



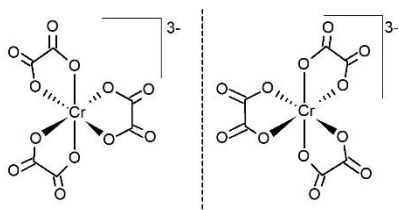
e) cis and trans:



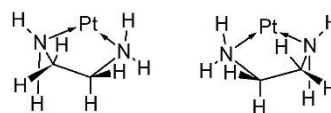
7.15



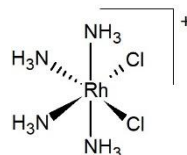
7.16 a) Chiral



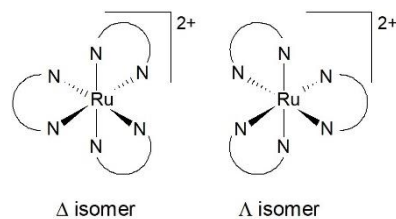
b) Chiral due to non-planarity of the five membered chelate ring:



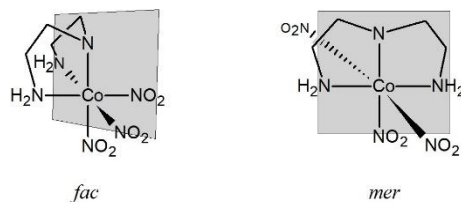
c) non-chiral, the mirror plane is the equatorial plane in the structure below:



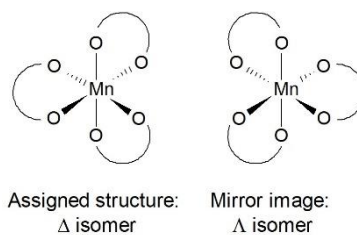
d) Chiral



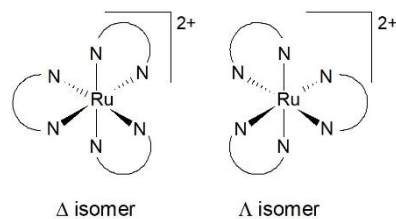
e) and f) neither is chiral,



7.17



7.18



- 7.19** The coordination geometry is changing, from stable square plane to five coordinate.
- 7.20** Chelating effect: bidentate ligands form more stable complexes than equivalent monodentate ligands.

Chapter 8

Self-Tests

- 8.1** The XRD pattern for CrO_2 will show identical reflections to those of rutile but shifted to slightly higher diffraction angles.
- 8.2** a) Higher intensity X-ray source is needed because the crystal is too small.
b) Neutrons are scattered from the nuclei, while X-rays from electrons; low electron density at H atoms leads to shorter H-element bonds.
- 8.3** TiO_2 has a strong absorbance in the UV region.
- 8.4** XeF_2 is a linear molecule with four vibrational modes.
- 8.5** a) ^{19}F NMR should consist of a quintet and a doublet in 1 : 4 intensity ratio.
b) The hydride resonance is split into a doublet through coupling to ^{103}Rh , then this is split into a doublet of doublets by one ^{31}P followed by splitting into a doublet of doublets of doublets by the second ^{31}P nucleus.
- 8.6** a) Three signals: one for SiO_4^{4-} and two for linear $\text{Si}_3\text{O}_{10}^{8-}$.
b) One signal.
- 8.7** The signal should be split into two lines due to ^{183}W isotope.
- 8.8** Below 0.2 mm s^{-1}

- 8.9** Gradual increase in energy of XAS K-edge as sulfur's oxidation state increases.
- 8.10** Both Cl and Br have isotopes that differ in mass for two mass units.
- 8.11** The hydrogen percentage is going to be lower for compounds containing heavier 5d metals decreasing the accuracy of the analysis.
- 8.12** The elements are close in the periodic table with similar electronic energies.
- 8.13** SnO_2 .
- 8.14** One reversible peak is expected.

Exercises

- 8.1** The reaction is complete when the diffraction pattern shows only the reflections due to the product.
- 8.2** X-ray powder diffraction.
- 8.3** For synchrotron source $0.5 \mu\text{m} \times 0.5 \mu\text{m} \times 0.5 \mu\text{m}$, for neutron source $500 \mu\text{m} \times 500 \mu\text{m} \times 500 \mu\text{m}$.
- 8.4** Low electron density at H atom positions, electrons associated with H atoms are shifted towards more electronegative N atom.
- 8.5** For a) X-ray could be helpful since the structure has only light elements; in case of b) neutron diffraction if a large crystal is obtained.
- 8.6** a) $\lambda = 152 \text{ pm}$; it is useful
b) 791 m/s .
- 8.7** The X-ray analysis always underestimates element-hydrogen bond lengths because of very low electron density at H nucleus. This is not an issue with neutron diffraction because neutrons will be scattered by

hydrogen nucleus giving a very accurate location.

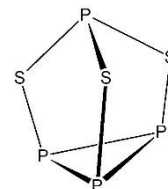
The C–H bond is of low polarity and the bonding pair is more equally distributed between the two nuclei so we would expect to see less discrepancy between X-ray diffraction and neutron diffraction with measurement of C–H bonds.

- 8.8** $\text{N}(\text{SiH}_3)_3$ is planar and thus N is at the centre of the molecule and does not move in the symmetric stretch. $\text{N}(\text{CH}_3)_3$ is pyramidal and the N–C symmetric stretch involves displacement of N.
- 8.9** When SCN^- binds to the metal through S atom, the C–S bond order decreases from 2 to 1 resulting in a lower vibration frequency (around 750 cm^{-1}). In $\text{RbBi}(\text{SCN})_4$ thiocyanate binds through S based on the given frequency.
- 8.10** 2404 cm^{-1} .
- 8.11** The bond orders for CN^- and CO are the same, but N is lighter than O, hence the reduced mass for CN^- is smaller resulting in a higher frequency. The bond order for NO is 2.5, and N is heavier than C. For the carbide anion we should expect the highest frequency because of the triple C–C bond and lightest carbon atoms.
- 8.12** O_2^+ has a higher bond order and should show in the region of 1800 cm^{-1} of Raman spectrum.
- 8.13** ^{19}F NMR should consist of two doublets of triplets; ^{77}Se NMR should have a triplet of triplets.
- 8.14** Two F atoms are axial; two chlorine and remaining F atom are equatorial in the trigonal bipyramidal structure.
- 8.15** The structure is pentagonal planar and all F atoms are magnetically equivalent, hence the strong central peak. The “flanking” peaks are due to the coupling to ^{129}Xe ($I = 1/2$, abundance 26.5%). The

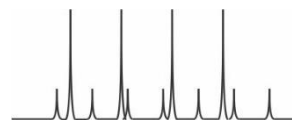
^{129}Xe NMR should have one sextet due to the coupling to five equivalent F nuclei.

- 8.16** XeF_3^+ is a T-shaped cation. ^{129}Xe NMR is a doublet of triplets resulting from the coupling to two equivalent F nuclei and one unique F nucleus. ^{19}F NMR has two signals one triplet (coupling to two F nuclei) and a doublet (coupling to one F nucleus), each is flanked by ^{129}Xe satellites.
- 8.17** The compound is fluxional at room temperature; cooling the sample down produces distinct signals for bridging and terminal CO groups.
- 8.18** PCl_5 in a solid state is an ionic compound: $[\text{PCl}_4]^+[\text{PCl}_6]^-$.

8.19

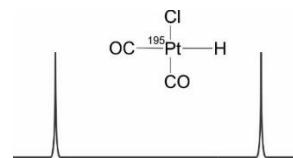


8.20 a)

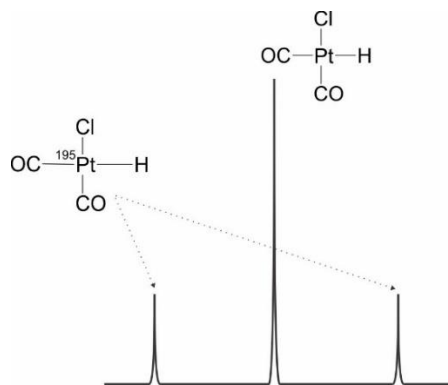


b)

^{195}Pt NMR:



^1H NMR (next page)



- 8.21** 1.95, 1.74 and 1.56.
- 8.22** EPR is more sensitive.
- 8.23** The Jahn–Teller effect distorts the structure from octahedral to tetragonal bipyramidal, when this effect is dynamic, the three directions are fluctuating at room temperature averaging the Cu–N bond lengths resulting in isotropic spectrum; on cooling the rate of exchange slows down to below the EPR time-scale and anisotropy is observed.
- 8.24** Room temperature: molecular tumbling is fast removing effect of g -value anisotropy; expect derivative-type spectrum, possibly exhibiting hyperfine structure that is centred at the average g value.
Frozen solution: g -value anisotropy can be observed, averaging from molecular tumbling does not apply.
- 8.25** Below $+0.2 \text{ nm s}^{-1}$.
- 8.26** If the iron centres have different oxidation states we should expect unique isomer shifts for each. Observing two distinct patterns suggests that the compound contains both Fe(III) and Fe(V).
- 8.27** The near edge structure can differentiate between different oxidation states and geometries making the interpretation of the spectrum easier.

- 8.28** The octahedral $[\text{Co}(\text{H}_2\text{O})_6]^{2+}$ is converted to tetrahedral $[\text{CoCl}_4]^{2-}$ upon addition of HCl.
- 8.29** ^{108}Ag silver isotope does not exist.
- 8.30** 258, 230, 200, 186, and 173.
- 8.31** $n = 7$.
- 8.32** yes.
- 8.33** The complex undergoes a reversible one electron reduction at $+0.21 \text{ V}$; one irreversible oxidation above $+0.720 \text{ V}$.
- 8.34** Part of the amorphous glass sample crystallized at 500°C .
- 8.35** acac-to- Co^{3+} ratio is 3 : 1.
- 8.36** a) it would be unsymmetrical
b) a peak would show with double intensity in comparison to the peaks in the figure.
- 8.37** SEM, TEM and light scattering methods.
- 8.38** $\text{Cu}_9\text{Zn}_5\text{Sn}_2\text{S}_{32}$; increase in mass.

Chapter 9

Self-Tests

- 9.1** Cd, Pb in sulfides; Rb and Sr aluminosilicates; Cr and Pd oxides and sulfides
b) As a sulfide.
- 9.2** a) VO_2^+
b) Mn^{2+} .
- 9.3** a) Longer oxygen chains are unlikely due to a strong O=O bond
b) The enthalpy of π component of a double bond decreases going down a group.
- 9.4** a) The enthalpy of vaporization decreases down a group. The increase in size of the central atom makes formation of

compounds with higher coordination number more favourable.

b) average $B(\text{Te-F}) = 358 \text{ kJ mol}^{-1}$.

9.5 the products (and their thermodynamic data formed) upon thermal decomposition for P_4O_{10} .

9.6 a) XeO_4 is tetrahedral, OsO_4
b) Ti; TiO_2 .

Exercises

9.1 (a) Ba, +2; (b) As, +5; (c) P, +5; (d) Cl, +7; (e) Ti, +4; (f) Cr, +6.

9.2 Group 2.

9.3 Group 15.

9.4 Group 6.

9.5 Second ionization energy for Na is too high.

9.6 Bi prefers +3 over +5 oxidation state, heavier halogens (Br and I) form stable +5 compounds; in group 16 Po would prefer +4 oxidation state.

9.7 Metallic character and ionic radii decrease across a period and down a group. Ionization energy increases across a period and decreases down a group. Large atoms typically have low ionization energies and are more metallic in character.

9.8 a) Be b) C c) Mn

9.9 a) Na b) O

9.10 a) LiH saline b) SiH_4 molecular
c) B_2H_6 molecular d) UH_3 saline
e) PdH_x metallic

9.11 a) Na_2O basic b) P_2O_5 acidic c) ZnO amphoteric
d) SiO_2 acidic e) Al_2O_3 amphoteric
f) MnO basic.

9.12 $\text{CrF}_2 < \text{CrF}_3 < \text{CrF}_6$

9.13 a) magnesite

b) bauxite

c) galena

d) magnetite

9.14 Z + 8 is V; stable OS +5 both like to form discrete and polymeric oxoanions.

9.15 Z + 22 is Hf; have oxides MO_2 , fluorides MF_4 and chlorides MCl_4 , +2 OS less stable than +4.

9.16 For SeF_6 , $262.5 \text{ kJ mol}^{-1}$; for SeF_4 , $348.7 \text{ kJ mol}^{-1}$.

9.17 NF_3 , -293 kJ mol^{-1} ; NCl_3 472 kJ mol^{-1} .
Strong Cl-Cl bond and a weak N-Cl bond contribute to instability of NCl_3 .

Chapter 10

Self-Tests

10.1 BiH_3

10.2 GeH_4 both

10.3 a) $\text{Ca(s)} + \text{H}_2\text{(g)} \rightarrow \text{CaH}_2\text{(s)}$.
b) $\text{NH}_3\text{(g)} + \text{BF}_3\text{(g)} \rightarrow \text{H}_3\text{N-BF}_3\text{(g)}$.
c) no reaction.

10.4 227 kJ mol^{-1}

10.5

$\text{Et}_3\text{SnH} + 2\text{Na} \rightarrow 2\text{Na}^+ \text{Et}_3\text{Sn}^- + \text{H}_2$
 $2\text{Na}^+ \text{Et}_3\text{Sn}^- + \text{CH}_3\text{Br} \rightarrow \text{MeEt}_3\text{Sn} + \text{NaBr}$.

Exercises

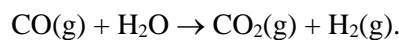
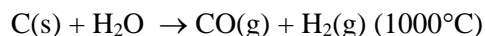
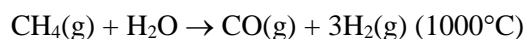
10.1 a) Hydrogen in Group 1: Hydrogen has one valence electron and is stable as H^+ .
b) Hydrogen in Group 17: Hydrogen can fill its 1s orbital and make a hydride H^- . Hydrides are isoelectronic with He. Group 1 and Group 2 metals, as well as transition metals, stabilize hydrides. The halogens are diatomic gases just like hydrogen, so

physically hydrogen would fit well in Group 17.

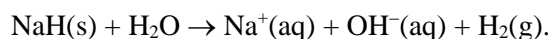
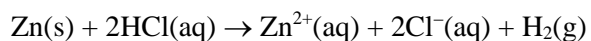
c) Hydrogen in Group 14: All elements in Group 14 are half way to obtaining the octet. Hydrogen has only one electron and thus is half way toward obtaining a stable electronic configuration of its corresponding noble gas, He. The addition of hydrogen to Group 14 would add a gaseous non-metal to the group producing a gradual change of the properties to non-metallic (but solid) carbon, then somewhat more metallic solid silicon all the way to purely metallic lead. However, none of these reasons are compelling enough to warrant placing hydrogen in Group 14.

- 10.2** a) H +1, S -2
b) K +1, H -1
c) Re +7, H -1
d) H +1, S +6, O -2
e) H +1, P +1, O -2.

10.3 Industry:



Laboratory



- 10.4** a) See Figure 10.2
b) See Figure 10.3 and data in Table 10.1
c) Group 13 electron-deficient, Group 14 electron precise and Groups 15, 16 and 17 electron-rich.

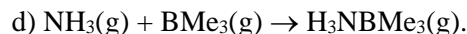
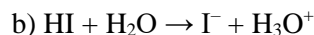
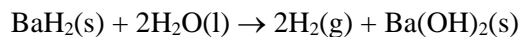
10.5 A gas with boiling point at -50°C or below, ice would be denser than liquid water.

10.6 O-H...S is stronger.

- 10.7** a) barium hydride, saline
b) silane, electron-precise molecular

- c) ammonia (azane), electron-rich molecular hydride
d) arsane (arsine), electron-rich molecular hydride
e) palladium hydride, metallic
f) hydrogen iodide, electron-rich molecular hydride.

10.8 a)



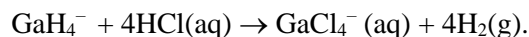
10.9 BaH_2 and $\text{PdH}_{0.9}$ solids, SiH_4 , NH_3 , AsH_3 and HI gases; $\text{PdH}_{0.9}$ might be a conductor.

10.10 For Group 1: increase in ionic radii of M^{+} increase the volume of the octahedral holes in the structure; Group 2 has no trend since the hydrides have variable structures.

10.11 reaction b).

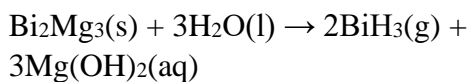
10.12 $(\text{CH}_3)_3\text{SnH}$ due to the weakest element-H bond.

10.13 GaH_4^{-} is the strongest reducing agent and most hydridic one



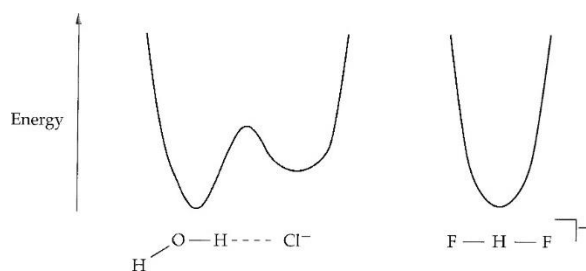
10.14 The period 2 hydrides, except for BeH_2 and B_2H_6 , are all exergonic. Their period 3 homologues either are much less exergonic or are endergonic. Period 2 compounds tend to be weaker Brønsted acids and stronger Brønsted bases than their period 3 homologues. The bond angles in period 2 hydrogen compounds reflect a greater degree of sp^3 -hybridization than the homologous period 3 compounds. As a consequence of hydrogen bonding, the boiling points of HF , H_2O , and NH_3 are all higher than their respective period 3 homologues.

10.15 BiH₃ is a very exothermic compound, expected to be less stable than SbH₃.
Methods of preparation:

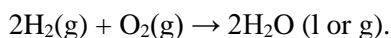
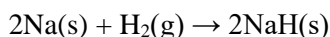


10.16 Clathrate hydrate is formed consisting of krypton atoms locked in cavities of ice structure.

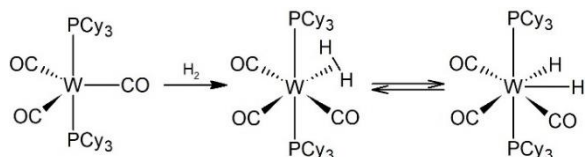
10.17



10.18 Hydrogen can exist in +1 and -1 oxidation states:



10.19



10.20

Incorrect: some p-block hydrides are not thermodynamically stable. In the second statement, the isotope of mass number 3 is radioactive, not of mass number 2.

Incorrect: not all hydrides of Group 2 are ionic; H⁻ is not compact

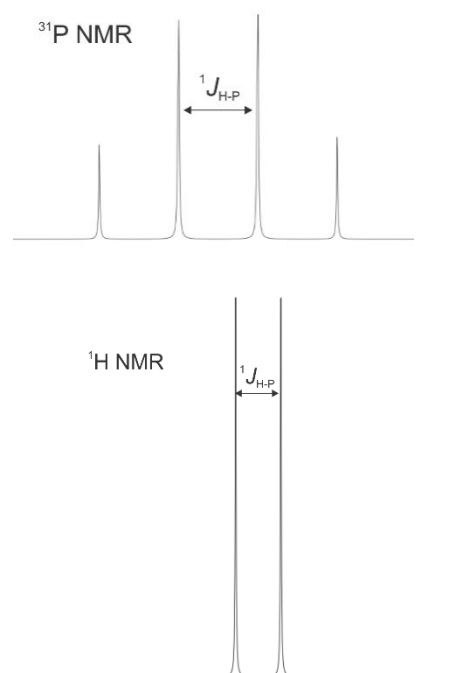
Incorrect: not all structures can be predicted by VSEPR theory, only those of electron-precise and electron-rich hydrides; this theory cannot explain B₂H₆, an electron-poor hydride.

Incorrect: NaBH₄ does not have greater hydridic character than a saline hydride.

Incorrect: boron hydrides are electron-deficient because they lack the electrons required to fill the bonding and non-bonding molecular orbitals.

10.21 2074 cm⁻¹.

10.22



Chapter 11

Self-Tests

11.1 NaCl-type structure.

11.2 Hydride anion must be very polarizable.

11.3 Yes.

11.4 LiF, 966.8 kJ mol⁻¹; CsF 713.9 kJ mol⁻¹; hydration energy for Li⁺ is insufficient to compensate for the lattice enthalpy

11.5 Increases down the group.

11.6 K₂SO₃.

11.7 K⁺ stabilizes NO₃⁻ in side the lattice better than Li⁺.

11.8 At low temperatures we should expect two peaks, at higher temperatures one averaged peak resulting from the mobility of Li^+ .

Exercises

- 11.1** a) Low first ionization potential
b) Low charge density, closed-shell electronic configuration.
- 11.2** The caesium-bearing silicate minerals are digested with sulfuric acid and Cs and Al are precipitated as alum $\text{Cs}_2\text{SO}_4 \cdot \text{Al}_2(\text{SO}_4)_3 \cdot 24\text{H}_2\text{O}$. The simple sulfate, obtained after roasting with carbon, is then converted to chloride using anion exchange. The isolated CsCl is then reduced with Ca or Ba.

11.3 Both CsCl type structure

11.4

	$-\Delta_f H^\circ / (\text{kJ mol}^{-1})$		$-\Delta_f H^\circ / (\text{kJ mol}^{-1})$
LiF	625	LiCl	470
NaF	535	NaCl	411
KF	564	KCl	466
RbF	548	RbCl	458
CsF	537	CsCl	456

For plot see Figure 11.6. The trends are related to the soft-hard preferences and ionic sizes.

- 11.5** Similarities are related to similar ionic radii.
- 11.6** Li^+ has a high hydration energy that compensates almost completely for the first ionization potential; little change would be expected with dimethyl sulfoxide, but increase in potential is expected in a weakly coordinating solvent.

11.7 a) etda^{4-} b) K^+

11.8 (i) A = LiOH; B = Li_2O ; C = none (Li_2O does not decompose); D = LiNH_2 .
(ii) A = RbOH; B = RbO_2 ; C = Rb_2O ; D = RbNH_2 .

11.9 $\text{CsO}_2 + \text{O}_3 \rightarrow \text{CsO}_3 + \text{O}_2$; liquid ammonia.

11.10 Solubility is lower if the cation and anion have similar radii.

11.11 FrI would likely have low solubility in water, Fr^+ can be precipitated with $[\text{Co}(\text{NO}_2)_6]^{3-}$ as insoluble $\text{Fr}_3[\text{Co}(\text{NO}_2)_6]$.

11.12 Small Li^+ and H^- result in a highly stable lattice, small Li^+ cannot stabilize quite large HCO_3^- .

11.13 For NaCl see Figure 11.4; for CsCl see Figure 11.5, Na^+ is smaller and requires smaller hole than Cs^+ .

11.14 Switch to CsCl structure type.

11.15 a) $\text{Li}(\text{CH}_3)_3 + \text{LiBr}$

b) $\text{Mg}(\text{C}_2\text{H}_5)_2\text{Br} + \text{LiCl}$

c) $\text{LiC}_6\text{H}_5 + \text{C}_2\text{H}_6$

11.16 Small alkyl groups lead to polymerization, bulkier groups produce monomers.

Chapter 12

Self-tests

12.1 No, best to use is sand or N_2 gas.

12.2 $[\text{BeCl}_2(\text{OEt}_2)_2]$

12.3 BeCl_2 is covalent; BaF_2 is ionic; BeCl_2 is polymeric, molecular; BaF_2 ionic crystal.

12.4 CaO 3465 kJ mol^{-1} , CaO_2 3040 kJ mol^{-1} . The trend is confirmed.

12.5 ZnS structure type.

12.6 $\text{BeSO}_4 \cdot 4\text{H}_2\text{O}$ would likely give $\text{Be}_2(\text{OH})_2(\text{SO}_4)$, $\text{SrBe}(\text{OH})_4$ gives SrO, BeO and H_2O .

12.7 MgF_2 2945 kJ mol^{-1} , MgBr_2 2360 kJ mol^{-1} , MgI_2 2193 kJ mol^{-1} ; we could expect that smallest halide, F^- , produces least soluble halide.

Exercises

12.1 Be is least electronegative and Be^{2+} has small radius, high charge density and high polarizing power.

12.2 Similar charge densities and electronegativities.

12.3 BeCl_2 is covalent, others are ionic

12.4 Intermetallic.

12.5 A = $\text{Ba}(\text{OH})_2$, B = BaCO_3 , C = BaC_2 , D = BaCl_2 .

12.6 Differences in structure, strong BeF_2 bonds are not completely broken during melting process.

12.7 $[\text{Be}(\text{NH}_3)_4]\text{F}_2$

12.8 Partial hydrolysis of $\text{Mg}^{2+}(\text{aq})$:
 $[\text{Mg}(\text{H}_2\text{O})_6]^{2+}(\text{aq}) + \text{H}_2\text{O}(\text{l}) \rightarrow$
 $[\text{Mg}(\text{OH})(\text{H}_2\text{O})_5]^+ + \text{H}_3\text{O}^+$

Ba^{2+} does not hydrolyze.

12.9 In BeH_2 18.2%, in MgH_2 7.6%; BeH_2 has low thermodynamic stability.

12.10 In general, Group 1 hydroxides have higher solubility in water and are stronger bases.

12.11 Gives two equivalents of OH^- , heavier, less hygroscopic.

12.12 MgSeO_4 .

12.13 44.6 billion tonnes.

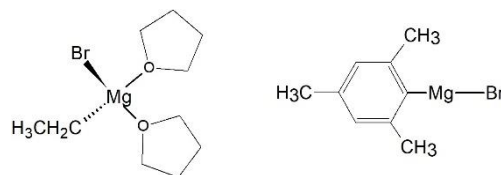
12.14 Precipitation using IO_4^- or TeO_4^{2-} .

12.15 Anhydrous MgSO_4 and CaSO_4 .

12.16 BeTe ZnS structure type; BaTe NaCl structure type

12.17 BeBr_2 covalent, MgBr_2 ionic, BaBr_2 ionic.

12.18 Bulky 2,4,6- $(\text{CH}_3)_3\text{C}_6\text{H}_2$ group reduces coordination number from four to two:



12.19 a) $\text{C}_2\text{H}_5\text{MgCl}$ b) $\text{Mg}(\text{C}_2\text{H}_5)$

c) $\text{C}_2\text{H}_5\text{MgCl}$

Chapter 13

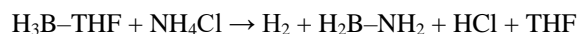
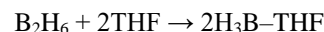
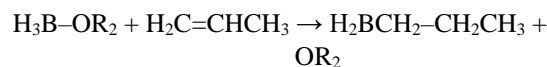
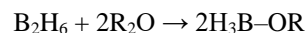
Self-tests

13.1 NH_2O

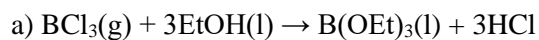
13.2 Face-centered lattice of Y^{3+} with $[\text{B}_{12}]^{2-}$ anions in octahedral holes.

13.3 Four lines of equal intensity

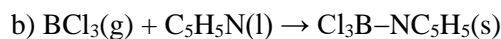
13.4



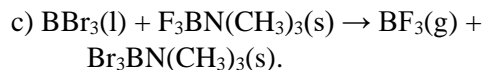
13.5



Similar to reaction with H_2O .

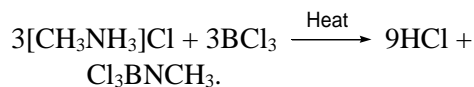


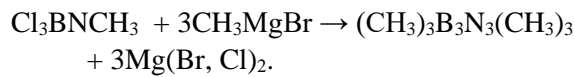
Lewis acid-base reaction.



BBr_3 is a stronger Lewis acid.

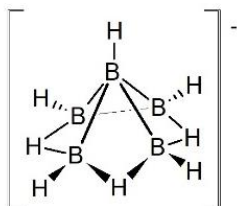
13.6



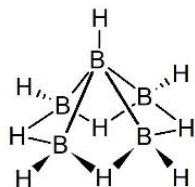


13.7 a) Seven electron pairs, arachno category.

b) Nido:



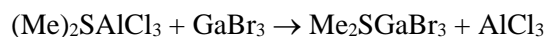
13.8 B_5H_9



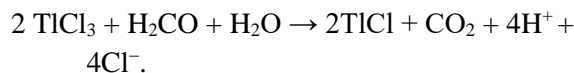
13.9 Closo structure, octahedron.

13.10

a) GaBr_3 is a softer Lewis acid:

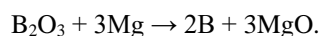
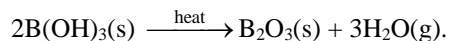
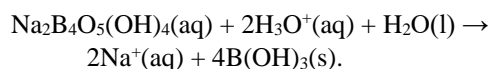


b) Tl(III) halides are unstable, oxidizing agents:



Exercises

13.1



13.2 It dissolves Al_2O_3 forming $[\text{AlF}_n]^{(3-n)+}$ species in the solution.

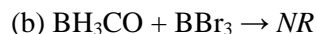
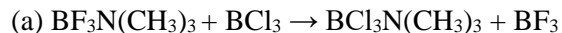
13.3 Al atoms in the formed amalgam can rapidly react with O_2 in air.

13.4 a) polar covalent bond

b) ionic

c) covalent

13.5 $\text{BCl}_3 > \text{BF}_3 > \text{AlCl}_3$.



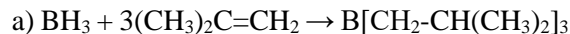
13.6 $\text{Na}^+[\text{TlBr}_4]^-$

13.7 A = B_2H_6 , B = $\text{B}(\text{OH})_3$, C = B_2O_3

13.8 No: $\text{B}_2\text{H}_6 + 3\text{O}_2 \rightarrow \text{B}_2\text{O}_3 + 3\text{H}_2\text{O}$ (one possibility).

13.9 a) Three b) Two

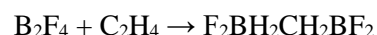
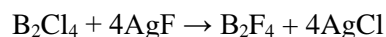
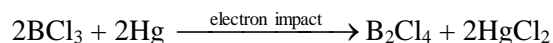
13.10



13.11 -73 172 kJ, B_2H_6 is very reactive, the combustion product is a solid.

13.12 Element–H bond enthalpy decreases down the group; Tl–H bond enthalpy is insufficient to compensate for other enthalpy expenses and TlH_3 is expected to be unstable.

13.13



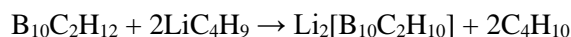
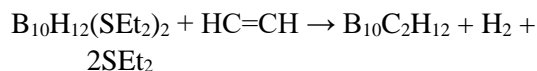
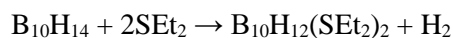
13.14 a) D_{2d} b) D_{2h} .

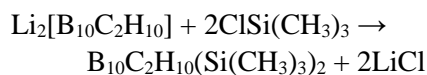
13.15 a) *nido*-decaborane(14)

b) dodecahydro-*closo*-dodecaborate(2-)

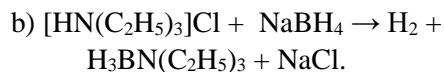
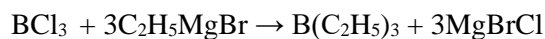
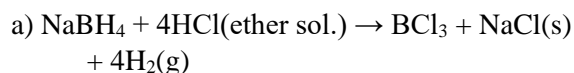
c) *Arachno*-tetradecahydrododecaborate(2-) or tetradecahydro-*arachno*-dodecaborate(2-)

13.16

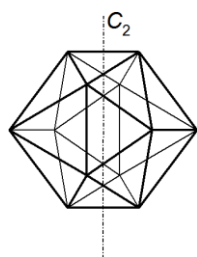




13.17



13.18



13.19 B₆H₁₀.

13.20 14 skeletal electrons or seven skeletal electron pairs.

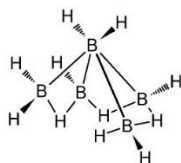
13.21 a) *nido*

b) 12 skeletal electron pairs.

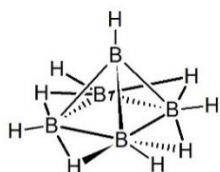
c) Number of valence electrons is $(10 \times 3) + (14 \times 1) = 44$. Ten $2c-2e$ B–H bonds account for 20 valence electrons, the number of cluster electrons is $44 - 20 = 24$.

13.22

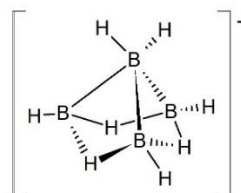
a)



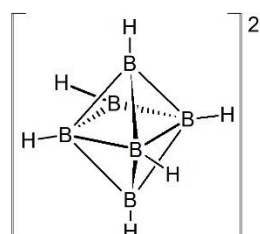
b)



c)



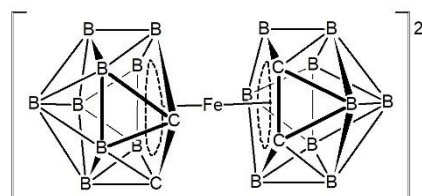
d)



13.23 B₆H₁₂, *arachno* structure.

13.24

- $\text{B}_{10}\text{H}_{14} + 2\text{SEt}_2 \rightarrow \text{B}_{10}\text{H}_{12}(\text{SEt}_2)_2 + \text{H}_2$
- $\text{B}_{10}\text{H}_{12}(\text{SEt}_2)_2 + \text{C}_2\text{H}_2 \rightarrow \text{B}_{10}\text{C}_2\text{H}_{12} + 2\text{SEt}_2 + \text{H}_2$
- $2\text{B}_{10}\text{C}_2\text{H}_{12} + 2\text{EtO}^- + 4\text{EtOH} \rightarrow 2\text{B}_9\text{C}_2\text{H}_{12}^- + 2\text{B}(\text{OEt})_3 + 2\text{H}_2$
- $\text{Na}[\text{B}_9\text{C}_2\text{H}_{12}] + \text{NaH} \rightarrow \text{Na}_2[\text{B}_9\text{C}_2\text{H}_{11}] + \text{H}_2$
- $2\text{Na}_2[\text{B}_9\text{C}_2\text{H}_{11}] + \text{FeCl}_2 \rightarrow 2\text{NaCl} + \text{Na}_2[\text{Fe}(\text{B}_9\text{C}_2\text{H}_{11})_2]$



13.25 a) one quartet

b) two doublets, intensity ratio 1 : 5.

13.26 Smaller size of B(III) dictates lower coordination numbers in comparison to Al(III).

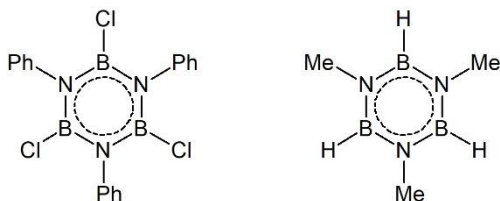
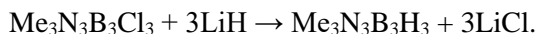
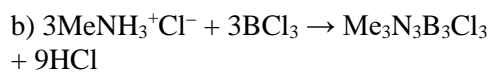
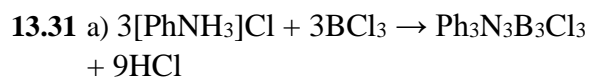
13.27 a) B(OH)₃ and HCl

b) [Cl₃BS(CH₃)₂].

13.28 Br is smaller than F and accommodating four large Br anions around relatively small B(III) is sterically challenging.

- 13.29** a) Both have layered structures. The planar sheets in BN and in graphite consist of edge-shared hexagons such that each B or N atom in BN has three nearest neighbours that are the other type of atom, and each C atom in graphite has three nearest neighbour C atoms. The structure of graphite is shown in Figure 14.2. The B–N and C–C distances within the sheets, are much shorter than the interplanar spacing. The B_3N_3 hexagonal rings are stacked directly over one another, whereas in graphite the C_6 hexagons are staggered.
- b) Graphite reacts with alkali metals and with halogens. In contrast, boron nitride is quite unreactive.
- c) The large HOMO–LUMO gap in BN, which causes it to be an insulator, suggests an explanation for the lack of reactivity: since the HOMO of BN is a relatively low-energy orbital, it is more difficult to remove an electron from it than from the HOMO of graphite, and since the LUMO of BN is a relatively high energy orbital, it is more difficult to add an electron to it than to the LUMO of graphite.

13.30 At high pressures and temperatures.



- 13.32** (a) is incorrect—in fact only boron has some non-metallic properties, all other elements are metallic.
- (b) is also incorrect—the hardness is decreasing down the group; in fact, of

Group 13 elements only boron and aluminium (top of the group) show pronounced oxophilicity and boron fluorophilicity.

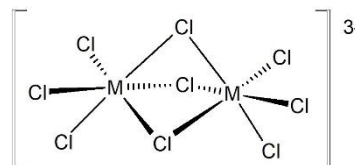
(c) is only partially correct—while Lewis acidity of BX_3 does increase from F to Br, it is not due to stronger B–Br π bonding (as stated) but exactly due to the opposite trend: the π bonding is decreasing in the same order Lewis acidity is increasing, that is, π bonding in B–Br is weaker than in B–F (the latter explains the former).

(d) is incorrect—*arachno* boron hydrides are less stable than *nido*-borohydrides, also, their skeletal electron count is $n + 3$ not $2(n + 3)$.

(e) is correct.

(f) is partially incorrect—while layered BN and graphite have similar structures, layered BN has a very large (not small as stated) HOMO–LUMO gap and is in fact an insulator (not a conductor as stated).

13.33



13.34 SiO_2

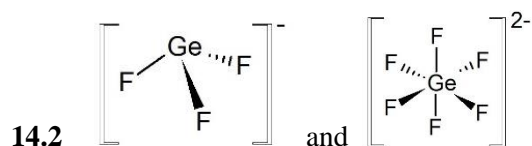
13.35 2.37 eV, 524 nm, yes.

13.36 Rb_2In_3 metallic bond; In_6^{4-} suggested to be octahedral as B_6^{2-} unit.

Chapter 14

Self-tests

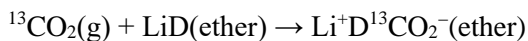
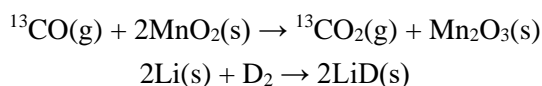
14.1 The temperature would decrease.



- 14.3 a) Chemical reductants donate their electrons to the LUMOs (graphite π^* MOs), resulting in a material with a higher conductivity.
 b) Chemical oxidants remove electrons from the HOMOs (π MOs) of graphite. This also results in a material with a higher conductivity.



14.5



- 14.6 Bond strength would decrease, bond length would increase.

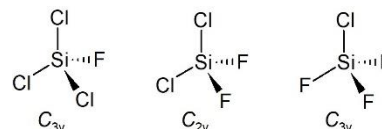
Exercises

- 14.1 (a) tin and lead are metallic elements.
 (b) is correct.
 (c) CS_2 is softer (not harder) than CO_2 .
 (d) zeolites are framework aluminosilicates (not layered like mica) and they do contain metal cations
 (e) is correct.
- 14.2 a) In the diamond-type structure, each atom forms single bonds with four neighbouring atoms located at the corners of a tetrahedron. Each atom in this structure can be seen as having sp^3 -hybridization and a full octet achieved through electron sharing in covalent bonds resulting in a wide energy gap smaller for Si(diamond) than for C(diamond).
 b) Carbon forms a rather stable monoxide, but silicon monoxide is an

unstable species. Both form very stable dioxides but while CO_2 is gas and a linear molecule, SiO_2 forms a network solid with Si–O–Si bridges, with each Si atom tetrahedrally surrounded with four O atoms throughout the structure.

c) Silicon tetrahalides are mild Lewis acids whereas analogous carbon compounds are not Lewis acidic. The reason for this difference in acidic properties is in the fact that silicon can extend its octet.

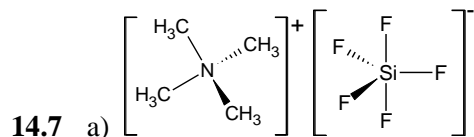
14.3



- 14.4 Ge has two easily accessible oxidation states: +2 and +4.

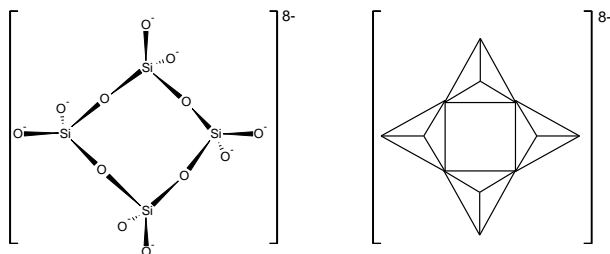
14.5 The bond enthalpy of a C–F bond is higher than the bond enthalpy of a C–H bond, making C–F bond more difficult to break. Further, the combustion of CH_4 produces not only CO_2 but H_2O as well, a very stable compound. Formation of both CO_2 and H_2O thermodynamically drive the combustion of CH_4 . There is no equivalent to the formation of H_2O in the combustion of CF_4 .

14.6 SiF_4 is a gas at standard conditions, while PbF_2 is a solid with two polymorphs. The electronegativity difference between Si and F is sufficiently large to indicate ionic bonding and thus a solid state structure. However, the atomic sizes and coordination in SiF_4 are the likely factors that prevent the lattice formation. Comparatively large and heavy Pb^{2+} can accommodate higher coordination numbers.



b) Two different magnetic environments: axial and equatorial.

14.8



14.9 a) doublet due to $^{119}\text{Sn}-^{31}\text{P}$ coupling

b) Central triplet ($^{31}\text{P}-^1\text{H}$ coupling) flanked by satellites ($^{119}\text{Sn}-^{31}\text{P}$ coupling).

14.10 For CCl_4 110 kJ mol^{-1} ; for CBr_4 86 kJ mol^{-1} .

14.11 A = SiCl_4 , B = SiRCl_3 (depends on the stoichiometry), C = RSi(OH)_3 , D = $\text{R(OH)}_2\text{SiOSi(OH)}_2\text{R}$, E = SiR_4 , F = SiO_2 .

14.12 a) +4 is the most stable oxidation state for the lighter elements, but +2 is the most stable oxidation state for Pb.

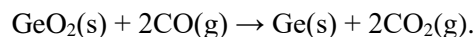
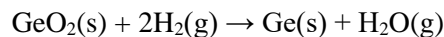
b) (i) $\text{Sn}^{2+} + \text{PbO}_2 + 4\text{H}^+ \rightarrow \text{Sn}^{4+} + \text{Pb}^{2+} + 2\text{H}_2\text{O}$; Pb^{2+} product more stable than Pb(IV) reactant

(ii) $2\text{Sn}^{2+} + \text{O}_2 + 4\text{H}^+ \rightarrow 2\text{Sn}^{4+} + 2\text{H}_2\text{O}$
 Sn^{4+} is more stable than Sn^{2+} on air.

14.13 Combining Pb^{4+} , an oxidizing agent, with a good reducing agent, I^- , will lead to a redox reaction and PbI_4 breaks down into PbI_2 and I_2 . On the other hand, since F_2 is one of the strongest oxidizing agents, F^- has virtually no reducing ability.

14.14 Silicon is a lithophile, lead is chalcophile element.

14.15 $\text{SiO}_2(\text{s}) + \text{C}(\text{s}) \rightarrow \text{Si}(\text{s}) + \text{CO}_2(\text{g})$



14.16 a) Band gap energy decreases down the group.

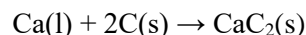
b) Increases, as Si is semiconductor.

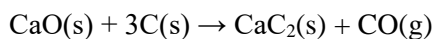
14.17

	Ionic carbides	Metallic carbides	Metalloid carbides
Group I elements	Li, Na, K, Rb, Cs		
Group II elements	Be, Mg, Ca, Sr, Ba		
Group 13 elements	Al		B
Group 14 elements			Si
3d elements		Sc, Ti, V, Cr, Mn, Fe, Co, Ni	
4d elements		Zr, Nb, Mo, Tc, Ru	
5d elements		La, Hf, Ta, W, Re, Os	
6d elements		Ac	
Lanthanides		Ce, Pr, Nd, Pm, Sm, Eu, Gd, Tb, Dy, Ho, Er, Tm, Yb, Lu	

14.18 a) Formed by heating graphite with potassium vapour or by treating graphite with a solution of potassium in liquid ammonia. The potassium atoms are oxidized to K^+ ions; their electrons are added to the LUMO π^* orbitals of graphite. The K^+ ions intercalate between the planes of the reduced graphite so that there is a layered structure of alternating sp^2 carbon atoms and potassium ions.

b) There are two methods: the direct reaction of the elements, and the reaction of calcium oxide with carbon:

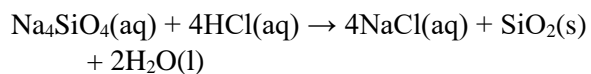
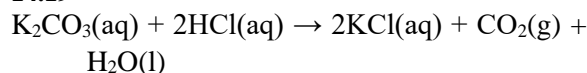




It contains discrete C_2^{2-} ions. The structure is similar to the NaCl structure, but because C_2^{2-} is a linear anion the unit cell is elongated in one direction making the unit cell tetragonal. This carbide is, hence, ionic.

c) A solution of C_{60} , in a high boiling point solvent (such as toluene), is treated with elemental potassium. It is also ionic, and it contains discrete K^+ ions and C_{60}^{3-} ions.

14.19



14.20 Small Si(IV) cannot accommodate six relatively large Cl^- .

14.21 The $[\text{SiO}_3^{2-}]_n$ ions in jadeite are a linear polymer of SiO_4 tetrahedra, each one sharing a bridging oxygen atom with the tetrahedron before it and the tetrahedron after it in the chain. In the two-dimensional aluminosilicate layers of kaolinite each silicon atom has three oxygen atoms that bridge to other silicon atoms in the plane, and one terminal oxygen atom.

14.22 Linear has two signals in 1 : 2 intensity ratio; cyclic only one signal.

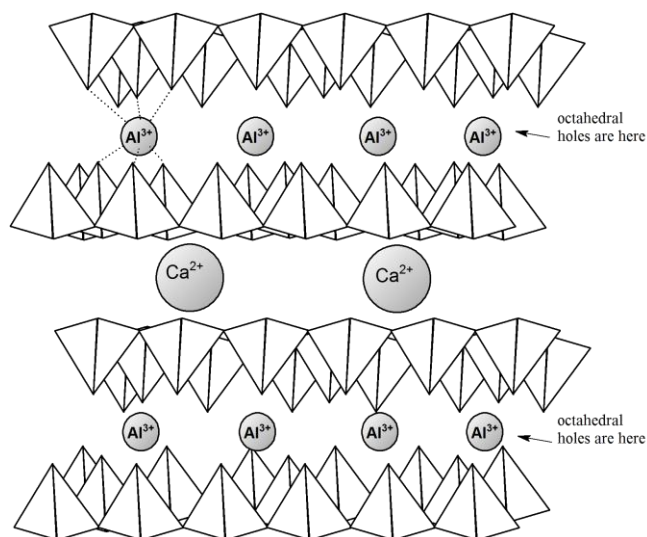
14.23 Both pyrophyllite, $\text{Al}_2\text{Si}_4\text{O}_{10}(\text{OH})_2$, and muscovite, $\text{KAl}_2(\text{Si}_3\text{Al})\text{O}_{10}(\text{OH})_2$, belong to the phyllosilicate subclass of silicate class. The phyllosilicates are characterized with two-dimensional sheets composed of vertex-sharing SiO_4 -tetrahedra; each SiO_4 -tetrahedron is connected to three neighbouring SiO_4 -tetrahedra via bridging O atoms. These sheets are negatively charged and held together via electrostatic interactions with cations sandwiched between the sheets. Because of this layered structure and

relatively weak electrostatic interactions keeping them together, both pyrophyllite and muscovite have excellent cleavage parallel to the layers (just like graphite). The hardness of the two minerals is, however, somewhat different—muscovite is harder than pyrophyllite (although both are very soft and can be scratched with a nail). The reason for this is in the chemical composition. Pyrophyllite layers are composed of exclusively SiO_4 tetrahedra held together with sandwiched Al^{3+} cations located in octahedral holes. In muscovite structure, however, every fourth Si^{4+} in the layer is replaced with Al^{3+} (see the formula— Si_3Al). The replacement of one +4 charge with +3 decreases the overall charge of layers and an additional cation is required to balance the charge. Strictly speaking one Si^{4+} is replaced with the $\text{Al}^{3+}/\text{K}^+$ pair. Lower charge on layers and more cations in between layers hold the muscovite structure tighter than pyrophyllite, and the result is higher hardness in muscovite.

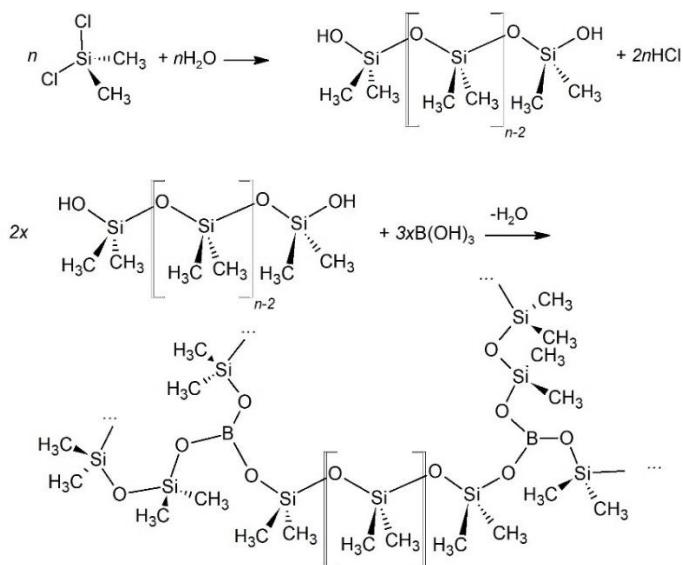
14.24 Glasses are amorphous silicon-oxygen compounds. Starting from sand (which is mostly pure SiO_2) and other oxide additives, a wide variety of glasses with different properties can be obtained, used and seen every day.

Activated carbon (used as adsorbent), carbon fibres (used as additives in plastic to increase the strength), and carbon black (used as pigment) are three examples of amorphous and partially crystalline carbon.

14.25 Al^{3+} that does not substitute for Si^{4+} can be found in octahedral holes between the layers. Larger Ca^{2+} is found in larger holes with coordination number 12.



14.26



Chapter 15

Self-Tests

15.1 $-3021 \text{ kJ mol}^{-1}$.

15.2 a) linear b) bent

15.3 a) Yes

b) Prediction is a triple bond, resulting in a stable molecule and gaseous form.

15.4 a) Weakening of element–H bond and stabilization of the lone pair (inert pair effect)

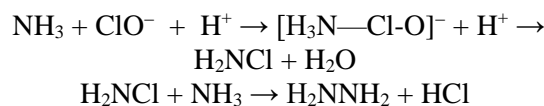
b) Formation enthalpy for NF_3 is negative (-209 kJ mol^{-1}) while that of NCl_3 is very positive (472 kJ mol^{-1}).

15.5 It is a liquid and does not have to be pressurized to be converted into a liquid state that takes less volume than gas. Unlike hydrocarbons, it does not produce CO_2 .

15.6 Sulfur is better oxidizing agent.

15.7 a) N_2O unreactive for kinetic reasons, NO is easily oxidized, NO_2 unreactive in air.

b) Hydrazine



Both steps could be seen as redox reactions.

Hydroxylamine: The reaction employed to synthesize hydroxylamine, which produces the intermediate $\text{N}(\text{OH})(\text{SO}_3)_2$, probably involves the attack of HSO_3^- (acting as a Lewis base) on NO_2^- (acting as a Lewis acid), although, because the formal oxidation state of the N atom changes from +3 in NO_2^- to +1 in $\text{N}(\text{OH})(\text{SO}_3)_2$, this can also be seen as a redox reaction. Whether one considers reactions such as these to be redox reactions or nucleophilic substitutions may depend on the context in which the reactions are being discussed. It is easy to see that these reactions do not involve simple electron transfer, such as in $2\text{Cu}^+(\text{aq}) \rightarrow \text{Cu}^0(\text{s}) + \text{Cu}^{2+}(\text{aq})$.

15.8 Four phosphate groups.

Exercises

15.1

	Type of element	Diatomic gas?	Achieves maximum oxidation state?	Displays inert pair effect?
N	nonmetal	yes	yes	no
P	nonmetal	no	yes	no
As	nonmetal	no	yes	no
Sb	metalloid	no	yes	no
Bi	metalloid	no	yes	yes

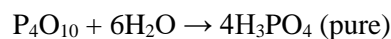
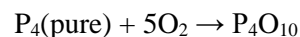
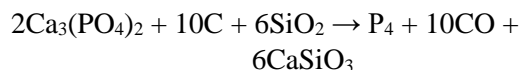
15.2 Moscovium is expected to be a metallic element, metallic radius 190–200 pm, I_1 probably 500 to 600 kJ mol⁻¹. Pauling's electronegativity 2.0–1.80. Preferred oxidation state would be +3, with +5 unstable and oxidizing. Its hydride, if stable at all, should have a formula McH₃, might be close to saline hydride. McH₅ is not expected to exist at all. The stable oxide is Mc₂O₃ with basic to amphoteric properties. Mc₂O₅ is a very strong oxidizing agent, with acidic properties. All halides for Mc(III) should be expected, McF₅ would be the only example of Mc(V) halides.

15.3 The bond enthalpy of N≡N bond is very large making N₂ molecule a preferred form for nitrogen. Any other allotrope would be based on N–N and N=N bonds, which are significantly weaker.

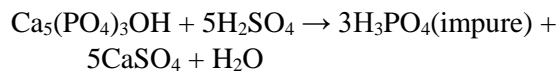
15.4 The cubic BN has a diamond-type structure with directional covalent bonds. The electrons in these bonds are very localized and cannot hop easily. The fact that boron and nitrogen are both rather electronegative elements further localize electrons around the bonds and atoms. The bonds in GaN are more polar, less localized and in combination with higher energies of Ga valence orbitals (and smaller energy difference between the orbitals in the valence shell in comparison

to boron) the band gap decreases. As we combine Ga with heavier Group 15 elements, the valence orbitals have better overlaps, are closer in energy and the band gap decreases. Decrease in electronegativity down the group also helps increase mobility of electrons and expansion of bands in the structure.

15.5 a)

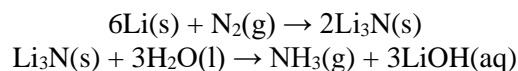


b)

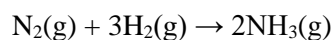


c) Fertilizer grade involves one step synthesis and no purification.

15.6 a)

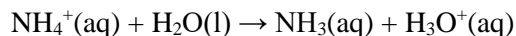
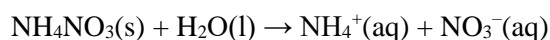


b)



c) Cost of lithium metal.

15.7



15.8 N₂ is non-polar, has lone electron pairs on more electro negative N atoms.

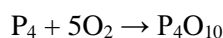
15.9 P is larger and better at reducing charge density, also the lone electron pair on P is higher in energy than the pair on N. Oxygen is very good at stabilizing high positive charges since it has a –2 charge itself.

15.10 NCl_3 is thermodynamically stable, NCl_5 does not exist; both PCl_3 and PCl_5 exist and are stable/

- 15.11** a) tetrahedral
 b) see-saw
 c) trigonal bipyramidal
 d) tetragonal pyramid
 e) octahedral

15.12 Inert electron pair in Bi(III) distorts the geometry.

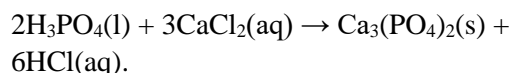
15.13 a)



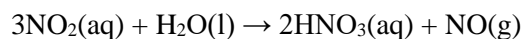
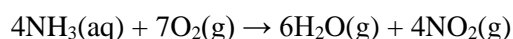
b)



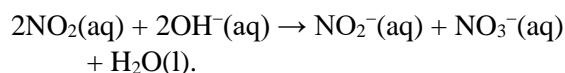
c) Calcium phosphate:



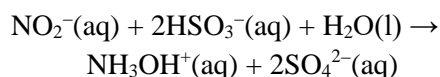
15.14 a)



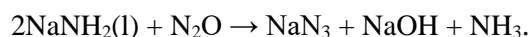
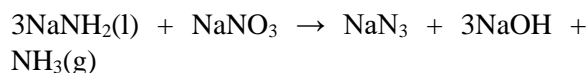
b)



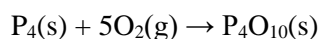
c)



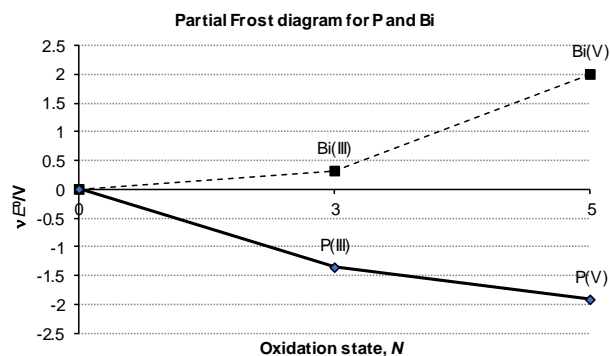
d)



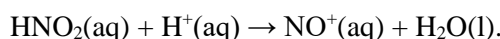
15.15 $\text{P}_4(\text{s})$ is not the most stable phase of phosphorus:



15.16 P(V) is the most stable oxidation state for this element, Bi(V) is the least stable oxidation state for Bi (oxidizing)



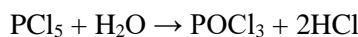
15.17 Decrease in pH increases the rate:



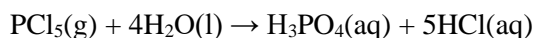
15.18 Reaction is more than first order in NO concentration.

15.19 $E_{\text{red}} = -0.736 \text{ V}$.

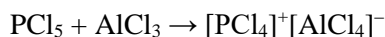
15.20 a)



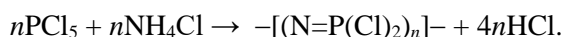
b)



c)



d)



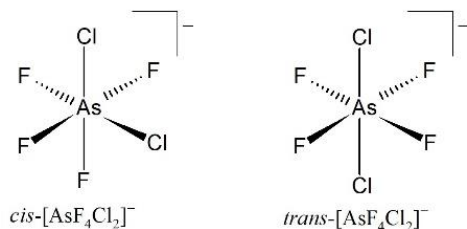
15.21 POCl_3 resonance is expected to be more downfield/

15.22 $E = +0.839 \text{ V}$; the anions are better reducing than oxidizing agents.

15.23 12 valence skeletal electrons or six skeletal electron pairs; *nido* structure derived from trigonal bipyramid.

15.24 A = AsCl_3 , B = AsCl_5 , C = AsR_3 , D = AsH_3

15.25 *Cis* isomer has two doublets, *trans* isomer has one singlet.



15.26 A = NO₂, B = HNO₃, C = NO, D = N₂O₄,
E = NO₂, F = NH₄⁺

15.27 The following can disproportionate: N₂O₄,
NO, N₂O, NH₃OH⁺, H₄P₂O₆, and P.

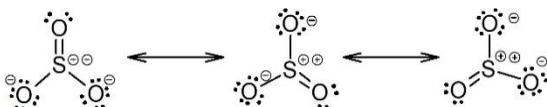
Chapter 16

Self-Tests

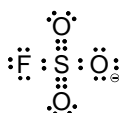
16.1 Bond order = 1.

16.2 It is spontaneous for both Br⁻ and Cl⁻.

16.3 a) D_{3h}



b) C_{3v}



16.4 S₄N₄ is aromatic.

Exercises

16.1 CO₂, P₄O₁₀, SO₃ are acidic, MgO, K₂O are basic, Al₂O₃ amphoteric, CO neutral.

16.2 For O₂ 1σ_g²1σ_u²2σ_g²1π_u⁴1π_g² and bond order = 2; for O₂⁺ 1σ_g²1σ_u²2σ_g²1π_u⁴1π_g¹ and bond order = 2.5, for O₂²⁻ 1σ_g²1σ_u²2σ_g²1π_u⁴1π_g⁴ and bond order = 1.

16.3 a) E = +1.068 V

b) No

c) D_rG = -157 kJ mol⁻¹, for H₂O₂ the value is -103 kJ mol⁻¹.

16.4 a) Incorrect: Se is not as easy to oxidize to Se(VI) as are S and Te.

b) The triplet state does not react as an electrophile.

c) Ozone pollution is unlikely to be caused by the diffusion from the stratosphere.

16.5 O-H...S

16.6 SF₆, -1329 kJ mol⁻¹; OF₆, -397 kJ mol⁻¹; SH₆, -456 kJ mol⁻¹; O in OF₆ and S in SH₆ are both in oxidation states inaccessible to these elements.

16.7 Ethylenediamine for both.

16.8 SO₃²⁻, SO₄²⁻, S₂O₈²⁻

16.9 All except +2.

16.10 a) H₅TeO₆ vs. HSO₄⁻ b) larger Te(VI) has higher coordination number than S(VI)—six vs. four.

16.11 S₂O₆²⁻ and S₂O₃²⁻.

16.12 Somewhat more stable in acidic solution

16.13 All will.

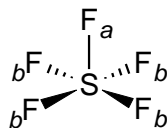
16.14 SF₃⁺ trigonal pyramidal, BF₄⁻ tetrahedral

16.15 The Frost diagram reveals that the stability of the lowest oxidation state is decreasing descending the group. Oxygen is very stable in oxidation state -2 and species containing oxygen in this state will be prevalent. Looking at the diagram overall, the same can be said for the other Group 16 elements: negative two oxidation state is the lowest on the diagram (besides the elemental form for all) and sulfides, selenides and tellurides should be the most stable compounds of these elements. Descending the group (starting with S already) positive oxidation states are accessible. All have good oxidizing properties. In the case of

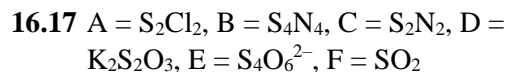
tellurium +4 and -2 have about the same stability. This is a consequence of the increased stability of higher oxidation states as we descend a group.



b)



c) One quintet, intensity 1 and one doublet intensity 4.



- 16.18 a) aromatic
b) aromatic
c) not aromatic

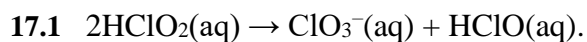
16.19 Sulfuric and selenic acids are rather similar. When pure, both are hygroscopic, very viscous liquids. Both form crystalline hydrates. Sulfuric and selenic acids react with their anhydrides, SO_3 and SeO_3 , to produce trisulfuric and triselenic acids respectively. Much like sulfuric acid, selenic acid is a strong acid in the first dissociation step, and the acids have the same order of magnitude for K_{a2} ($\sim 10^{-2}$). Both produce two types of salts: hydrogensulfates/sulfates and hydrogen-selenates/selenates. The salts also have similar solubilities. The most important difference between the two acids is their oxidizing power: H_2SeO_4 is a very strong oxidizing agent capable even of oxidizing gold and palladium.

Telluric acid is remarkably different from sulfuric and selenic acid. When pure, it is a solid composed of discrete $\text{Te}(\text{OH})_6$ octahedra. This structure is retained in the solution as well. As it can be expected, it forms more than two types of salts: H_5TeO_6^- , $\text{H}_4\text{TeO}_6^{2-}$, $\text{H}_2\text{TeO}_4^{4-}$, and TeO_6^{6-} . It is a weak acid even in the first dissociation step. At

elevated temperatures it loses water molecules to produce various polytelluric acids. What is similar to sulfuric and selenic acid is that $\text{Te}(\text{OH})_6$ can produce well-defined, crystalline hydrates. Telluric acid is a weaker oxidizing agent than selenic acid in both acidic and alkaline medium but is a stronger oxidant than sulfuric acid in either medium.

Chapter 17

Self-Tests



17.2 Linear

17.3 Both can be used but SO_2 is cheaper.

17.4 Bond order = 0.5; bond is longer.

17.5 A sextet, intensity 2 and a triplet intensity 5.

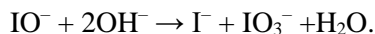
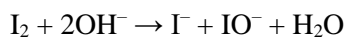
17.6 ClF_3 is T-shaped, SbF_5 is trigonal bipyramidal; ClF_2^+ is bent, SbF_6^- is octahedral.

17.7 For example: I_3^- , IBr_2^- , ICl_2^- , and IF_2^- .

17.8 a) Br_2 and BrO^-



b) I_2 and IO^-



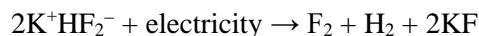
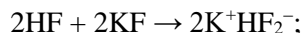
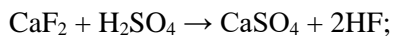
Exercises

17.1

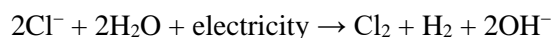
	Physical state	Electronegativity	Hardness of halide ion	Colour
F_2	gas	highest (4.0)	hardest	light yellow

Cl ₂	gas	lower	softer	yellow -green
Br ₂	liquid	lower	softer	dark red- brown
I ₂	solid	lowest	softest	dark violet

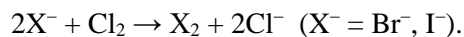
17.2 Fluorine:



Chlorine:



Bromine and iodine:



17.3 Bond order: 1.5, bond shorter.

17.4 See Figure 17.4; reaction is $2\text{OH}^-(\text{aq}) + \text{Cl}_2(\text{aq}) \rightarrow \text{ClO}^-(\text{aq}) + \text{Cl}^-(\text{aq}) + \text{H}_2\text{O}(\text{l})$

17.5 This orbital accepts the electron pair from Lewis base:

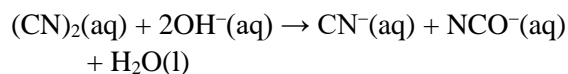


17.6 F₂ and Cl₂.

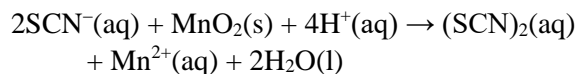
17.7 a) presence of hydrogen bond in NH₃

b) Electron withdrawing F atoms decrease the energy of nitrogen's lone pair.

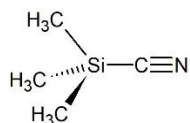
17.8 a)



b)



c)

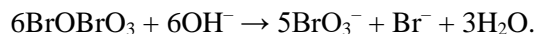


17.9 a) $[(\text{CH}_3)_4\text{N}][\text{IF}_4^-]$

b) IF₃ T-shaped, (CH₃)₄N⁺ tetrahedral, IF₄⁻ square planar

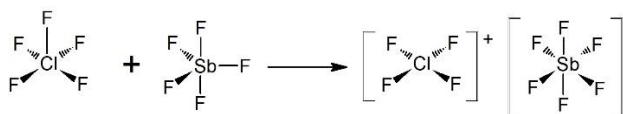
c) IF₃ has two resonances: a triplet of intensity 1 and a doublet of intensity 2; the product has only one resonance

17.10 BrO₂ or BrOBrO₃:

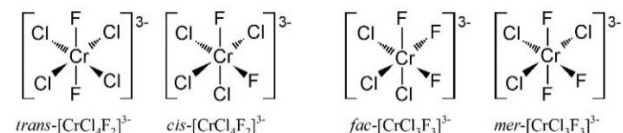


17.11 SbCl₅ trigonal bipyramid, FClO₃ tetrahedral

17.12

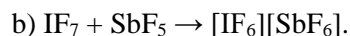


17.13

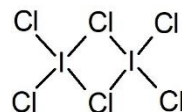


Trans and *cis* each have one resonance, *fac* also has one while *mer* has two: a doublet (intensity 2) and a triplet (intensity 1)

17.14 a) [IF₆]⁺ octahedral, IF₇ pentagonal bipyramidal



17.15 D_{2h}



17.16 Trigonal pyramidal, C_s

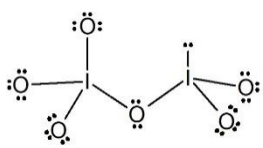
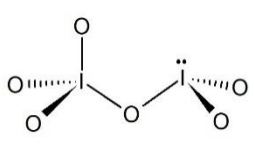
17.17 a) as a Lewis base

b) no effect

c) as a Lewis acid

17.18 Two different I-I bond lengths: longer central I-I distances (290 pm) and shorter terminal I-I distances (268 pm). The difference in bond lengths can be

explained by different bond order. This gives us one description of I_5^+ structure as a hybrid of two structures. The three-centre description is based on MO theory.

- 17.19** Two resonances: a doublet (intensity 4) and a quintet (intensity 1).
- 17.20** a) Since SbF_5 cannot be oxidized, it will not form an explosive mixture with BrF_3 .
 b) Methanol, being an organic compound, is readily oxidized by strong oxidants.
 c) The two will not form an explosive mixture but will react.
 d) S_2Cl_2 will be oxidized to higher valent sulfur fluorides.
- 17.21** $Br_3^- + I_2 \rightarrow 2IBr + Br^-$.
- 17.22** Larger Cs^+ stabilizes I_3^- better than smaller Na^+ .
- 17.23** a) bent geometry, C_{2v} .
 b) C_s
- 

- 17.24** a) $HBrO_4$ (stronger acid) and H_5IO_6 .
 b) H_5IO_6 is more stable.
- 17.25** a) E decreases with increase in pH (Figure 17.14)
 b) $E = 0.788$ V, less positive than at pH = 0.
- 17.26** Low pH results in a kinetic promotion: protonation of an *oxo* group aids oxygen-halogen bond scission.
- 17.27** a) +0.45 V b) +0.67 V c) +0.317 V.
- 17.28** a) $HClO$, $HClO_2$, and ClO_3^- are unstable with respect to disproportionation.

b) The rates of disproportionation are probably $HClO > HClO_2 > ClO_3^-$.

- 17.29** a) Yes b) No c) No d) Yes
- 17.30** a) Yes b) Yes c) Yes d) No
- 17.31** A = ClF ; B = OF_2 ; C = HF ; D = SiF_4 ; E = $CsClF_2$; G = CaF_2 .
- 17.32** a) BrO_4^- is capable of oxidizing water. This makes preparation and isolation of $KBrO_4$ very difficult.
 b) All compounds are kinetically reasonably stable to be isolated.
 c) IO_2^- ion is too unstable for its salts to be isolated.
 d) BrO^- and IO^- are disproportionating too rapidly to be isolated.
- 17.33** a) Correct
 b) Incorrect - the two anions do not have identical structures.
 c) Incorrect - it is the nucleophilicity of the Cl atom in ClO^- that is crucial for the oxidation mechanism.
 d) Correct.

Chapter 18

Self-Tests

- 18.1** Bond order = 1.
- 18.2** -408 kJ mol $^{-1}$.
- 18.3** $2HXeO_4^-(aq) + 2OH^-(aq) \rightarrow XeO_6^{4-}(aq) + Xe(g) + O_2(g) + 2H_2O(l)$.

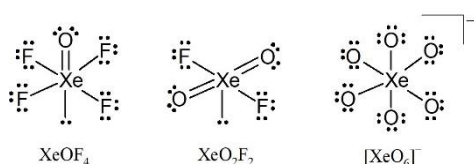
Exercises

- 18.1** Earth's gravitational field is not strong enough to hold light gases such as He and H_2 , and they eventually diffuse away into space.
- 18.2** a) He b) Xe c) Ar

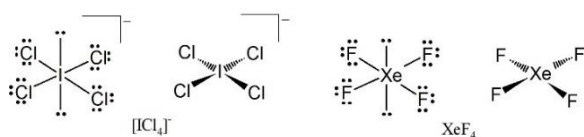
- 18.3 a) $\text{Xe}(\text{g}) + \text{F}_2(\text{g}) \rightarrow \text{XeF}_2(\text{s})$.
 b) $\text{Xe}(\text{g}) + 3\text{F}_2(\text{g}) \rightarrow \text{XeF}_6(\text{s})$
 c) $\text{XeF}_6(\text{s}) + 3\text{H}_2\text{O}(\text{l}) \rightarrow \text{XeO}_3(\text{s}) + 6\text{HF}(\text{g})$.

18.4 -133 kJ mol^{-1} .

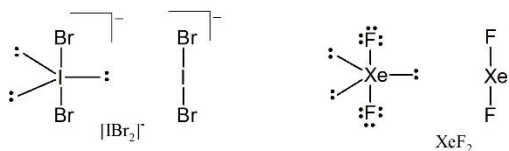
18.5



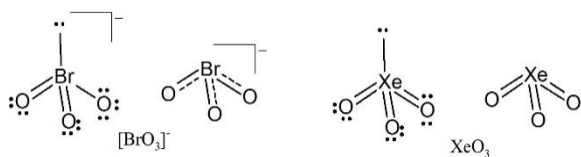
18.6 a)



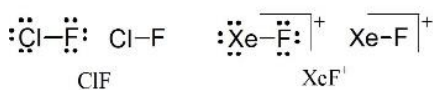
b)



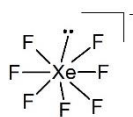
c)



d)

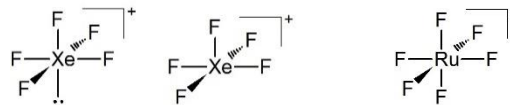


18.7 a)



b) capped octahedral

18.8



18.9 Both have bond order 0.5.

- 18.10 a) trigonal planar
 b) T-shaped
 c) square pyramid
 d) pentagonal planar.

18.11 A = XeF_2 ; B = $[\text{XeF}][\text{MeBF}_3]$; C = XeF_6 ;
 D = XeO_3 ; E = XeF_4 .

18.12 A singlet flanked by a doublet satellite

18.13 One quartet

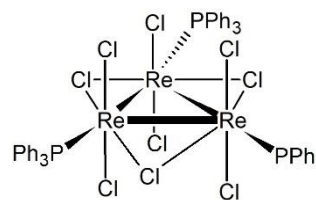
18.14 One singlet with a doublet satellite.

Chapter 19

Self-tests

19.1 V_2O_3 is more stable than VO .

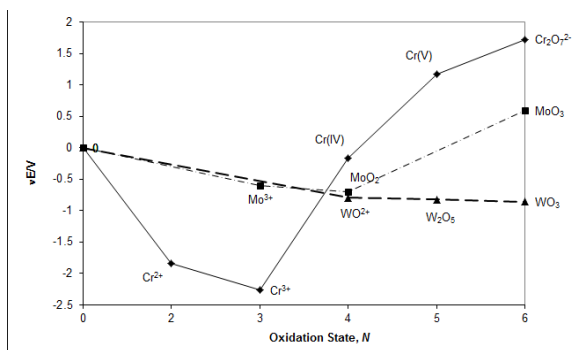
19.2



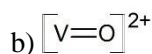
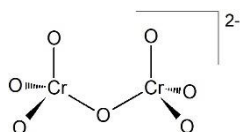
Exercises

19.1 +7 for Mn, MnO_4^- ; +8, the stability is increasing down the group.

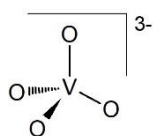
- 19.2 a) +6 for Cr and Mo; W has none
 b) Cr, Cr(IV) and Cr(V)



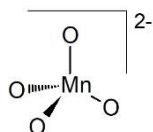
19.3 a)



c)



d)



19.4 Oxidation states for Fe and Co are not stable, very strong oxidizing agents

19.5 a) Correct

b) correct

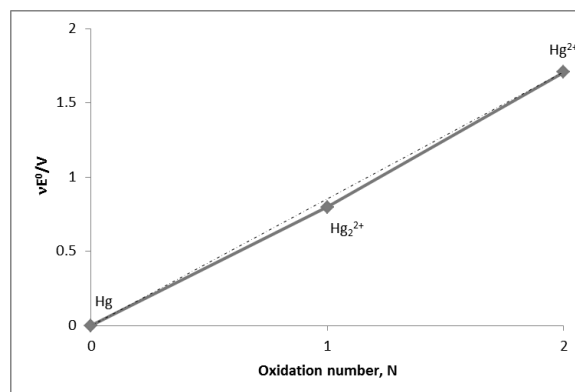
c) incorrect

d) correct.

19.6 RbAu and CsAu are likely to be the only stable ones.

19.7 Ionic radii are almost identical but Hf is heavier than Zr.

19.8 Hg_2^{2+} will not disproportionate



19.9 Stable to atmosphere, not light sensitive, low vapour pressure, good coverage ability, non-toxic, easy and cheap extraction and/or easy and cheap synthesis.

Chapter 20

Self-tests

20.1 High-spin $-0.8\Delta_o$, low-spin $-1.8\Delta_o + P$.

20.2 $t_{2g}^3 e_g^2$.

20.3 LFSE for FeF_2 , CoF_2 and NiF_2 increases the stability of the lattice.

20.4 In the spectrum of $[Mo(CO)_6]$, the ionization energy around 8 eV was attributed to the t_{2g} electrons that are largely metal-based. The differences in the 6–8 eV region can be attributed to the lack of d electrons for Mg(II).

20.5 1F and 3F .

20.6 a) 3P b) 2D

20.7 3F terms are $^3T_{1g}$, $^3T_{2g}$ and $^3A_{2g}$; 1D terms are $^1T_{2g}$ and 1E_g .

20.8 $17\,500\text{ cm}^{-1}$ and $22\,400\text{ cm}^{-1}$.

20.9 The low intensity band is due to the spin- and Laporte forbidden transition $^2E_g \leftarrow ^4A_{2g}$; bands at $17\,700\text{ cm}^{-1}$ and $23\,800\text{ cm}^{-1}$ correspond to the $^4T_{2g} \leftarrow ^4A_{2g}$ and $^4T_{1g} \leftarrow ^4A_{2g}$ transitions, respectively; the strong band at $32\,400\text{ cm}^{-1}$ is MTLC.

Exercises

- 20.1** a) t_{2g}^6 ; $-2.4\Delta_o + 2P$
 b) $t_{2g}^4 e_g^2$; $-0.4\Delta_o$
 c) t_{2g}^5 ; $-2.0\Delta_o + 2P$
 d) t_{2g}^3 ; $-1.2\Delta_o$
 e) t_{2g}^6 ; $-2.4\Delta_o + 2P$
 f) $e^3 t_2^3$; $-0.6\Delta_T$
 g) $e^4 t_2^6$; $0\Delta_T$.

20.2 No. A complex can develop a large value of Δ_o : with π -acidic ligands or with strongly σ -basic ligands (or both).

20.3

Complex	N	$\mu/\mu_B = [(N)(N + 2)]^{1/2}$
$[\text{Co}(\text{NH}_3)_6]^{3+}$	0	0
$[\text{Fe}(\text{OH}_2)_6]^{2+}$	4	4.9
$[\text{Fe}(\text{CN})_6]^{3-}$	1	1.7
$[\text{Cr}(\text{NH}_3)_6]^{3+}$	3	3.9
$[\text{W}(\text{CO})_6]$	0	0
$[\text{FeCl}_4]^{2-}$	4	4.9
$[\text{Ni}(\text{CO})_4]$	0	0

20.4 3.8 for $[\text{Cr}(\text{H}_2\text{O})_6]^{3+}$; 0 for CrO_4^{2-} ; 1.8 for $[\text{Fe}(\text{CN})_6]^{3-}$ and 5.9 for $[\text{Fe}(\text{H}_2\text{O})_6]^{3+}$.

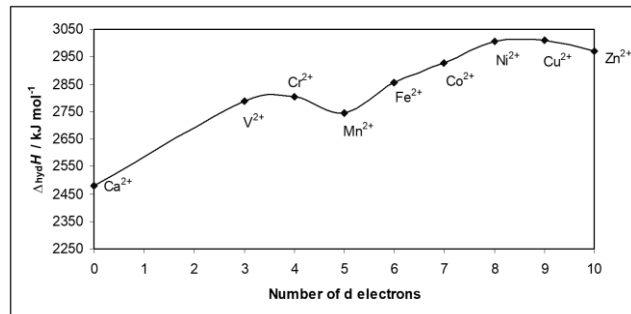
20.5 $[\text{CoCl}_4]^{2-}$ is blue, $[\text{Co}(\text{NH}_3)_6]^{2+}$ is yellow, $[\text{Co}(\text{OH}_2)_6]^{2+}$ is pink.

- 20.6** a) The Cr complex
 b) The Fe^{3+} complex
 c) $[\text{Fe}(\text{CN})_6]^{3-}$
 d) The Ru complex
 e) The Co^{2+} complex.

20.7 LFSE for Ti^{2+} , V^{2+} , Fe^{2+} , Co^{2+} and Ni^{2+} are non-zero and they contribute to the stability of the oxides.

20.8

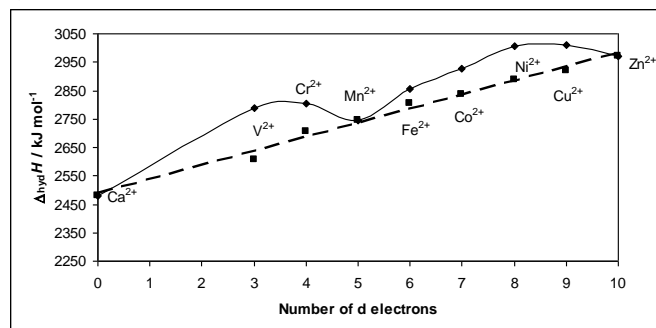
a)



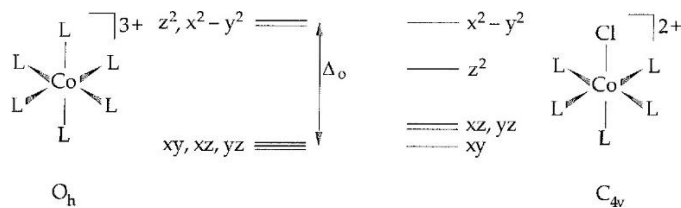
b)

Ion	Ca^{2+}	V^{2+}	Cr^{2+}	Mn^{2+}	Fe^{2+}	Co^{2+}	Ni^{2+}	Cu^{2+}	Zn^{2+}
Δ_o (in cm^{-1})	0	12600	13900	7800	10400	9300	8300	12600	0
Δ_o (in kJ mol^{-1})	0	150.5	166.1	93.2	124.2	111.1	99.2	150.5	0
$t_{2g} e_g$ config.	$t_{2g}^0 e_g^0$	$t_{2g}^3 e_g^0$	$t_{2g}^3 e_g^1$	$t_{2g}^3 e_g^2$	$t_{2g}^4 e_g^2$	$t_{2g}^5 e_g^2$	$t_{2g}^6 e_g^2$	$t_{2g}^6 e_g^3$	$t_{2g}^6 e_g^4$
LFSE (kJ mol^{-1})	0	-180.6	-99.6	0	-49.7	-88.9	-119	-90.3	0

c)



- 20.9** Shift from square planar to tetragonal complex
- 20.10** Distorted octahedral/tetragonal bipyramidal.
- 20.11** Due to the degeneracy of the excited e_g state, the “single” electronic transition is really the superposition of two transitions, one from an O_h ground-state ion to an O_h excited-state ion, and a lower energy transition from an O_h ground-state ion to a lower energy distorted excited-state ion.
- 20.12** a) 6S b) 4F c) 2D d) 3P
- 20.13** a) 3F b) 5D c) 6S
- 20.14** a) 6S b) 1D , 3P (ground term), 1S
- 20.15** $B = 861.33 \text{ cm}^{-1}$, $C = 3\,167.7 \text{ cm}^{-1}$.
- 20.16** a) d^6 , $^1A_{1g}$
 b) d^1 , $^2T_{2g}$
 c) d^5 , $^6A_{1g}$.
- 20.17** a) $\Delta_o = 8\,500 \text{ cm}^{-1}$; $B = 770 \text{ cm}^{-1}$
 b) $\Delta_o = 10\,750 \text{ cm}^{-1}$; $B = 720 \text{ cm}^{-1}$.
- 20.18** $\epsilon > 10^4 \text{ dm}^3 \text{ mol}^{-1} \text{ cm}^{-1}$ MnO_4^-
 $\epsilon = 100 \text{ dm}^3 \text{ mol}^{-1} \text{ cm}^{-1}$ $[\text{CoCl}_4]^{2-}$
 $\epsilon = 10 \text{ dm}^3 \text{ mol}^{-1} \text{ cm}^{-1}$ $[\text{Co}(\text{H}_2\text{O})_6]^{2+}$
 $\epsilon < 1 \text{ dm}^3 \text{ mol}^{-1} \text{ cm}^{-1}$ $[\text{Fe}(\text{H}_2\text{O})_6]^{3+}$.
- 20.19** The presence of two moderate-intensity bands in the visible/near-UV spectrum of $[\text{Co}(\text{NH}_3)_6]^{3+}$ suggests that it is low spin. The very weak band in the red corresponds to a spin-forbidden transition such as $^3T_{2g} \leftarrow ^1A_{1g}$.
- 20.20** No spin-allowed transitions are possible for the Fe^{3+} ; the complex is expected to be colorless. The $d^6 \text{Co}^{3+}$ ion in $[\text{CoF}_6]^{3-}$ is also high spin, but in this case a single spin-allowed transition makes the complex colored and gives it a one-band spectrum.
- 20.21** The bonding between Co^{3+} and the ligand has more covalent character in $[\text{Co}(\text{CN})_6]^{3-}$ than in $[\text{Co}(\text{NH}_3)_6]^{3+}$.
- 20.22** The intense band, with $\epsilon_{\text{max}} = 2 \times 10^4 \text{ M}^{-1} \text{ cm}^{-1}$, at relatively high energy is both a spin- and Laporte allowed LMCT transition. The two bands with $\epsilon_{\text{max}} = 60$ and $80 \text{ M}^{-1} \text{ cm}^{-1}$ are probably spin-allowed but Laporte-forbidden ligand field (d–d) transitions. The very weak band with $\epsilon_{\text{max}} = 2 \text{ M}^{-1} \text{ cm}^{-1}$ is most likely a spin-forbidden ligand field (d–d) transition.
- 20.23** The faint green color, which is only observed when looking through a long pathlength of bottle glass, is caused by spin-forbidden ligand field transitions.
- 20.24** The blue-green colour of the Cr^{3+} ions is caused by spin-allowed but Laporte-forbidden ligand field transitions. The relatively low-molar-absorption coefficient is the reason that the intensity of the colour is weak. The oxidation state of chromium in tetrahedral chromate dianion is Cr(VI), which is d^0 . Therefore, no ligand field transitions are possible. The intense yellow colour is due to LMCT transitions.
- 20.25** The d_{z^2} orbital has A_1 symmetry. The Cl– lone electron pairs can form π molecular orbitals with d_{xz} and d_{yz} . These metal atomic orbitals are π -antibonding MOs in $[\text{CoCl}(\text{NH}_3)_5]^{2+}$ and so they will be raised in energy relative to their position in $[\text{Co}(\text{NH}_3)_6]^{3+}$, in which they were degenerate with d_{xy} . Since Cl^- ion is not as strong a σ -base as NH_3 is, the d_{z^2} orbital in $[\text{CoCl}(\text{NH}_3)_5]^{2+}$ will be at lower energy than in $[\text{Co}(\text{NH}_3)_6]^{3+}$, in which it was degenerate with $d_{x^2-y^2}$.



20.26 The oxidation state of manganese in permanganate anion is Mn(VII), which is d^0 . Therefore, no ligand field transitions are possible.

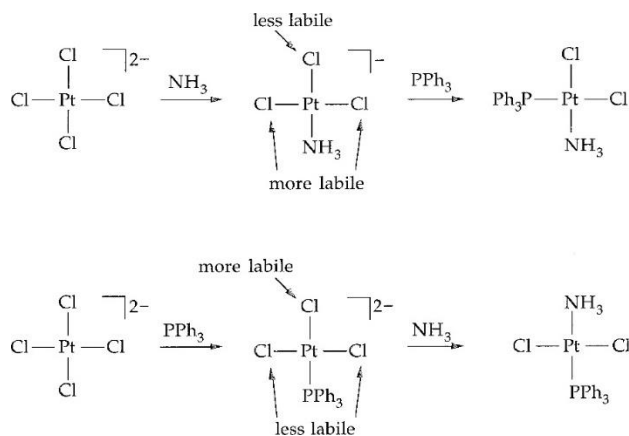
The difference in energy between the two transitions, $E(t_2) - E(e) = 13700 \text{ cm}^{-1}$, is just equal to Δ_T .

Chapter 21

Self-Tests

21.1 $k_2(\text{NO}_2^-) = 10^{0.71} = 5.1 \text{ dm}^3 \text{ mol}^{-1} \text{ s}^{-1}$.

21.2



21.3 $K_E = 1 \text{ dm}^3 \text{ mol}^{-1}$; $k_2 = 1.2 \times 10^2 \text{ s}^{-1}$.

Exercises

21.1 Dissociative.

21.2 The rate of an associative process depends on the identity of the entering ligand so it is not an inherent property of $[\text{M}(\text{OH}_2)_6]^{n+}$.

21.3 d

21.4 $\text{rate} = (kK_E[\text{Mn}(\text{OH}_2)_6^{2+}][\text{X}^-]) / (1 + K_E[\text{X}^-])$

By varying the nature of X^- : if k varies as X^- varies, then the reaction is a ; if not, then the reaction is d .

21.5 Metal centers with high oxidation numbers and those from period 5 and 6 in d-block have stronger bonds to ligands than metal centers with low oxidation numbers and period 3 d-block.

21.6 The greater steric hindrance.

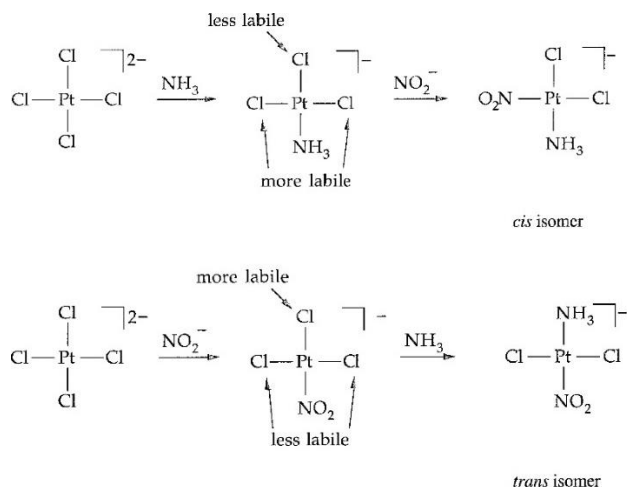
21.7 This is a case of dissociative activation.

21.8 Mechanism must be dissociative.

21.9 Yes. For a detectable amount of $[\text{Ni}(\text{CN})_5]^{3-}$ to build up in solution, the forward rate constant k_f must be numerically close to or greater than the reverse rate constant k_r .

21.10 A possible mechanism is loss of one dimethyl sulfide ligand, followed by the coordination of 1,10-phenanthroline.

21.11



21.12 a) Rate decreases.

b) The rate decreases.

c) The rate decreases.

d) Rate increase.

21.13 (i) The general trend: octahedral Co(III) complexes undergo dissociatively activated ligand substitution.

(ii) The anomalously high rate of substitution by OH⁻ signals an alternate path, that of base hydrolysis.

(iii) The implication is that a complex without protic ligands will not undergo anomalously fast OH⁻ ion substitution.

21.14 a) *cis*-[PtCl₂(PR₃)₂].

b) *trans*-[PtCl₂(PR₃)₂].

c) *trans*-[PtCl₂(NH₃)(py)].

21.15 [Ir(NH₃)₆]³⁺ < [Rh(NH₃)₆]³⁺ < [Co(NH₃)₆]³⁺ < [Ni(OH₂)₆]²⁺ < [Mn(OH₂)₆]²⁺.

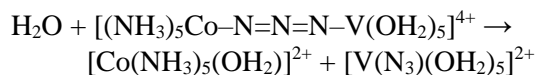
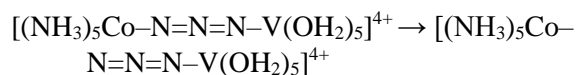
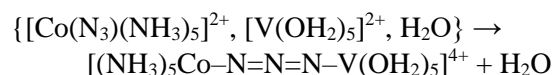
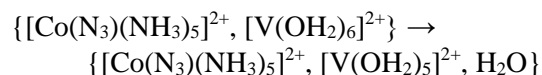
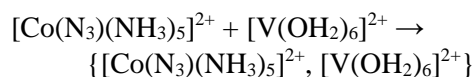
21.16 a) Decreased rate.

b) Decreased rate.

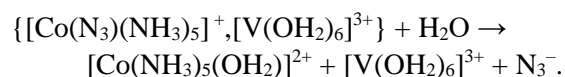
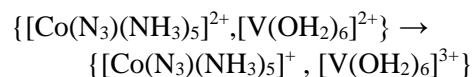
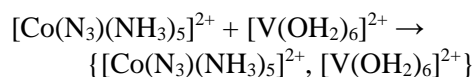
c) This change will have little or no effect on the rate.

d) Decreased rate.

21.17 Inner-sphere pathway:



Outer-sphere pathway:



Determining the fate of N₃⁻ ligand should reveal the actual pathway.

21.18 Appears to be an inner-sphere electron transfer reaction.

21.19 The reduction of [Co(NH₃)₅(OH)]²⁺ proceeds via inner-sphere mechanism. The [Co(NH₃)₅(H₂O)]³⁺ has no bridging ligands and the only mechanistic pathway for the electron-transfer is outer sphere. Both reactions with [Ru(NH₃)₆]²⁺ as a reducing agent likely proceed via the same mechanism, the outer-sphere mechanism.

21.20 a) $k = 4.53 \times 10^3 \text{ dm}^3 \text{ mol}^{-1} \text{ s}^{-1}$

b) $k = 1.41 \times 10^{-2} \text{ dm}^3 \text{ mol}^{-1} \text{ s}^{-1}$

The reduction of the Ru complex is more thermodynamically favoured and faster.

21.21 Ru couple $k_{12} = 2.95 \times 10^3 \text{ dm}^3 \text{ mol}^{-1} \text{ s}^{-1}$

Fe couple $k_{12} = 3.19 \times 10^7 \text{ dm}^3 \text{ mol}^{-1} \text{ s}^{-1}$

The second Ru couple $k_{12} = 8.51 \times 10^{15} \text{ dm}^3 \text{ mol}^{-1} \text{ s}^{-1}$.

21.22 The product will be [W(CO)₅(NEt₃)], and the quantum yield will be 0.4.

21.23 ~250 nm,

Chapter 22

Self-Tests

22.1 No.

22.2 Electron count 16, oxidation state +2.

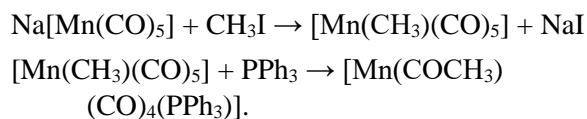
22.3 Dibromocarbonylmethyl-bis(triphenylphosphine)iridium(III).

22.4 [Fe(CO)₅]

22.5 a) $\eta^6\text{-C}_7\text{H}_8 = 6$ electrons, Mo atom = 6, carbonyl = 2 electrons, total = 18.

b) $\eta^7\text{-C}_7\text{H}_7^+ = 6$ electrons, Mo atom = 6, 3 COs = 6, total = 18.

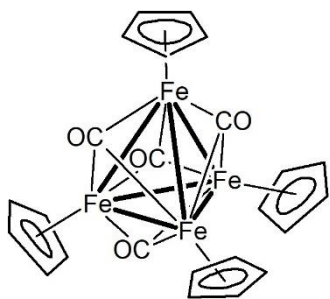
22.6 [Mn₂(CO)₁₀] + 2Na → 2Na[Mn(CO)₅]



22.7 Bridging.

22.8 It will not.

22.9



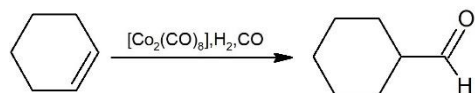
22.10 PMe_3 would be preferred, because of its smaller size.

22.11 Fluorenyl compounds are more reactive than indenyl.

22.12 The decrease in both coordination number and oxidation number by 2.

22.13 The ethyl group in $[\text{Pt}(\text{PEt}_3)_2(\text{Et})(\text{Cl})]$ is prone to β -hydride elimination.

22.14



22.15 The rate of catalysed hydroformylation reaction will decrease.

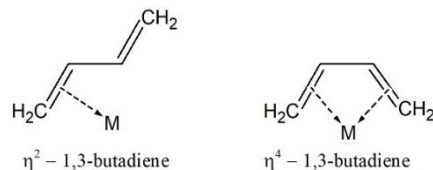
22.16 Without R groups attached to the Zr centre or geometric constraints by the ligands there is no preference for specific binding of new alkenes during polymerization and thus the repeat is random or atactic.

Exercises

- 22.1 a) Pentacarbonyliron(0)
b) Decacarbonyldimanganese(0)

- c) Hexacarbonylvandium(0)
 d) Tetracarbonylferrate(II)
 e) Tris(pentamethylcyclopentadienyl)-lanthanum(III)
 f) η^3 -allyltricarboxylchloridoiron(II)
 g) Tetracarbonyltriethylphosphineiron(0)
 h) Dicarboxylmethyltriphenylphosphine-rhodium(I)
 i) Chloridomethylbis(triphenylphosphine)-palladium(II)
 j) η^5 -cyclopentadienyl- η^4 -tetraphenylcyclobutadienecobalt(I)
 k) η^5 -cyclopentadienyldicarbonylferrate(0)
 l) η^6 -benzene- η^6 -cycloheptatrienechromium(0)
 m) Trichloridobis(η^5 -cyclopentadienyl)-tantalum(V)
 n) η^5 -cyclopentadienylnitrosylnickel(II).

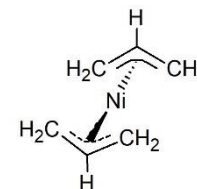
22.2



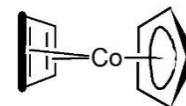
- 22.3 a) η^2 b) η^1, η^3, η^5 c) η^2, η^4, η^6
d) η^2, η^4

22.4

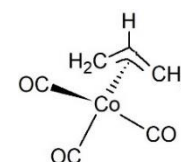
- a) 16, expected for d^8 electron config.



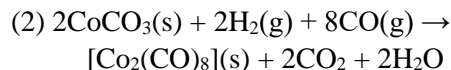
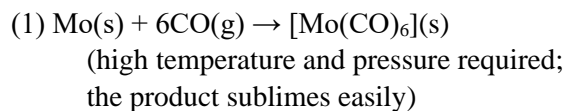
- b) 18



- c) 18



22.5



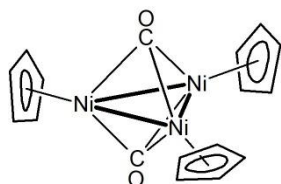
The reason that the second method is preferred is kinetic, not thermodynamic.

22.6 A complex that has C_s symmetry will have the greatest number of bands. A fragment with D_{3h} symmetry will give rise to one band, a fragment with C_{3v} symmetry will give rise to two bands, and a fragment with C_s symmetry will give rise to three bands.

22.7 a) CO bands of the trimethylphosphine complex are 100 cm^{-1} or more lower in frequency. PMe_3 is primarily a σ -donor ligand. PF_3 is primarily a π -acid ligand.

b) CO bands of the Cp^* complex are lower in frequency than the corresponding bands of the Cp complex. Cp^* is a stronger donor ligand than Cp .

22.8 a)



b) It does not follow 18 electron rule, but Ni is in the region where that is expected.

22.9 The Ir complex since it follows associative mechanism.

22.10 $[\text{Fe(CO)}_4]^{2-}$ due to a higher negative charge

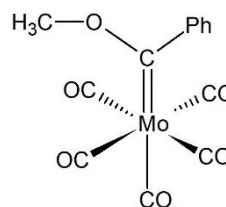
(b) The rhenium complex. The greater M-H bond enthalpy for a period 6 metal ion.

22.11 a) 3 b) 2 c) 12

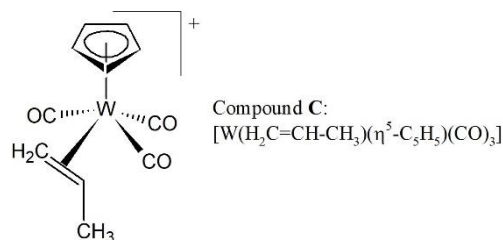
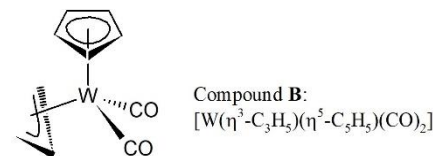
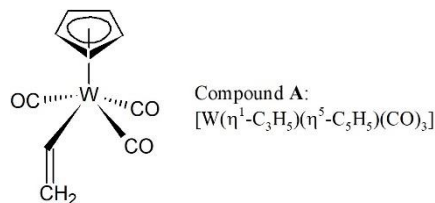
22.12 i) Reduce $[\text{Mn}_2(\text{CO})_{10}]$ with Na to give $[\text{Mn(CO)}_5]^-$; react this anion with MeI to give $[\text{MnMe(CO)}_5]$

b) Oxidize $[\text{Mn}_2(\text{CO})_{10}]$ with Br_2 to give $[\text{MnBr(CO)}_5]$; displace the bromide with MeLi to give $[\text{MnMe(CO)}_5]$.

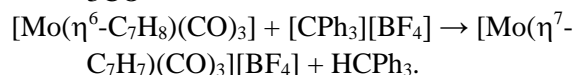
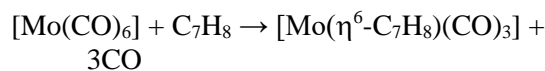
22.13



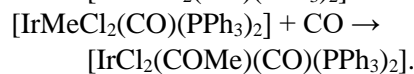
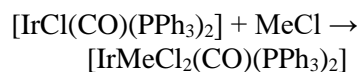
22.14



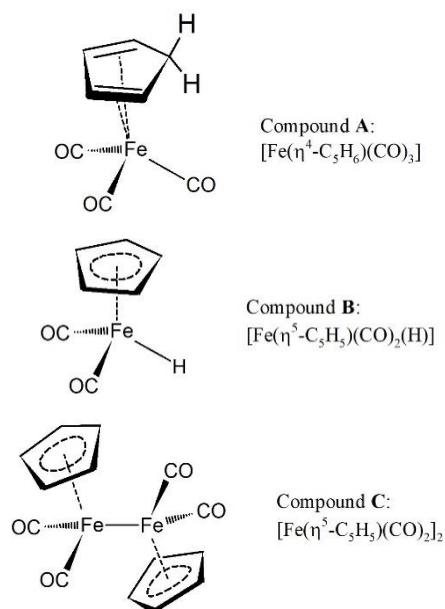
22.15 a)



b)

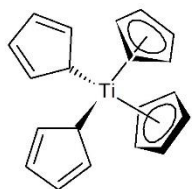


22.16

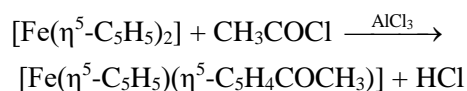


22.17 In either case compounds formed are tetraalkyl titanium(IV) complexes, TiR₄. Notice that neither the methyl nor trimethylsilyl groups have β hydrogens.

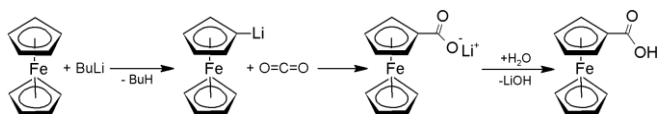
22.18 The fluxional structure shown below in which η¹ and η⁵ Cp⁻ ligands are scrambled explains the experimental observations.



22.19 a)



b)

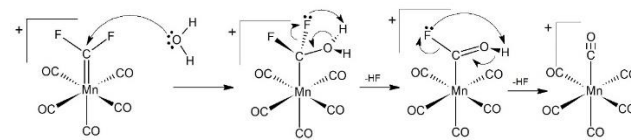


22.20 Consult Resource Section 5. On the metal the d_{z^2} and s orbitals have an a_1' symmetry and thus have correct symmetry

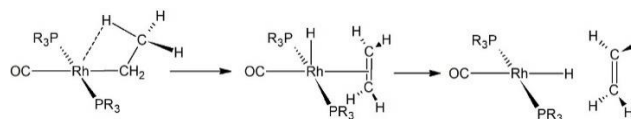
to form the MOs with the a_1' symmetry-adapted orbital on Cp rings. Other atomic orbitals on the metal do not have the correct symmetry. Therefore, three a_1' MOs will be formed. Figure 22.13 shows the energies of the three a_1' MOs.

22.21 Both [FeCp₂] and [FeCp₂H]⁺ are 18 electron species., [NiCp₂H]⁺ is a 20 electron species while [NiCp(η⁴-C₅H₆)]⁺ is an 18 electron species.

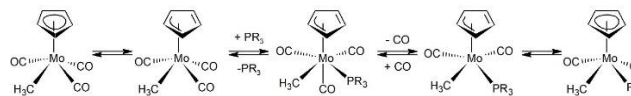
22.22 a)



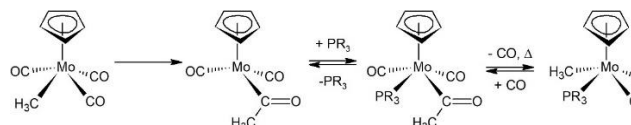
b)



22.23



Or



22.24 a) octahedral 86, trigonal prismatic 90

b) for octahedral no; for trigonal prismatic yes

c) The Fe compound is probably octahedral while the Co compound is probably trigonal prismatic

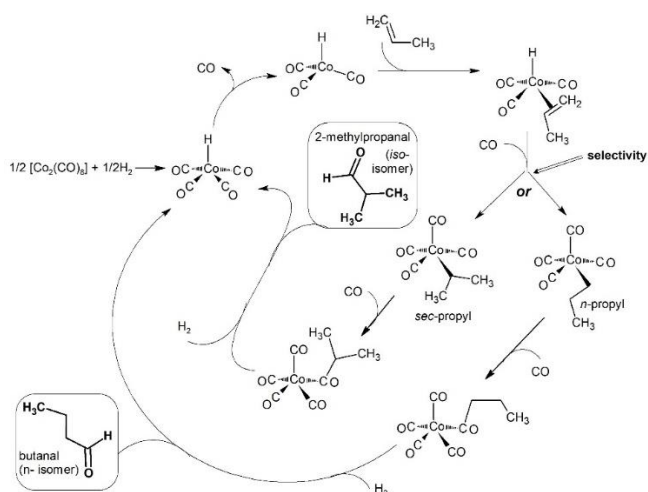
22.25 a) SiCH₃ b) I

22.26 Co compound because Co–Co bonds are weaker than Ir–Ir bonds if all other factors (such as geometry and ligand types) are kept the same.

22.27 Catalytically inactive complex **B** of Figure 22.18 becomes the predominant species.

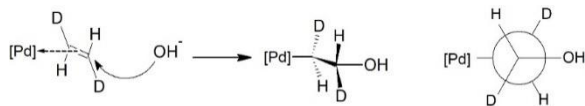
22.28 Steric hindrance around C=C double bond.

22.29

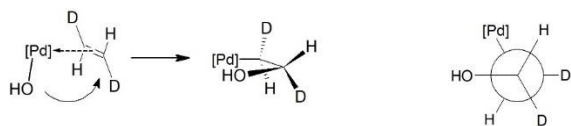


22.30 Since compound (E) in Figure 22.20 is observed under catalytic conditions, its formation must be faster than its transformation into products. The transformation of (E) into $[\text{CoH}(\text{CO})_4]$ and product must be the rate-determining step. In the presence of added PBU_3 , neither compound (E) nor its phosphine-substituted equivalent is observed, requiring that their formation must be slower than their transformation into products. Thus, in the presence of added PBU_3 , the formation of either (A) or (E), or their phosphine-substituted equivalents, is the rate-determining step.

22.31 a)

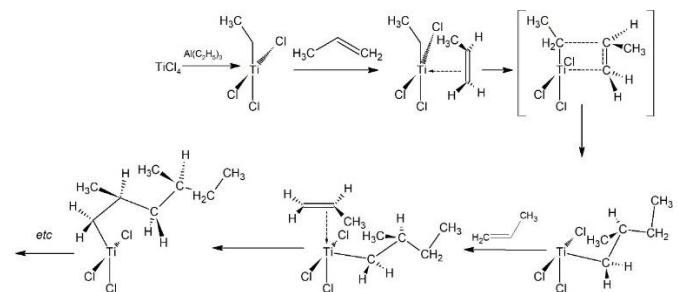


b)



c) Yes

22.32



Polymer is going to be isotactic.

Chapter 24

Self-Tests

23.1

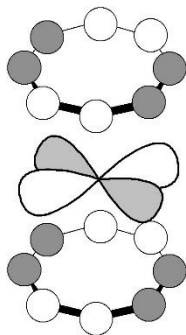
Ln	Pr	Nd	Pm	Dy	Ho	Er
El. Conf./ [Xe]	$4f^3 6s^2$	$4f^4 6s^2$	$4f^5 6s^2$	$4f^{10} 6s^2$	$4f^{11} 6s^2$	$4f^{12} 6s^2$
Ln^{2+}	Pr^{2+}	Nd^{2+}	Pm^{2+}	Dy^{2+}	Ho^{2+}	Er^{2+}
El. Conf./ [Xe]	$4f^3$	$4f^4$	$4f^5$	$4f^{10}$	$4f^{11}$	$4f^{12}$
Term	$4I_{9/2}$	$5I_4$	$6H_{5/2}$	$5I_8$	$4I_{15/2}$	$3H_6$
Ln^{3+}	Pr^{3+}	Nd^{3+}	Pm^{3+}	Dy^{3+}	Ho^{3+}	Er^{3+}
El. Conf./ [Xe]	$4f^2$	$4f^3$	$4f^4$	$4f^9$	$4f^{10}$	$4f^{11}$
Term	$3H_4$	$4I_{9/2}$	$5I_4$	$6H_{15/2}$	$5I_8$	$4I_{15/2}$
Change in L	Decrease	The same	Increase	Decrease	The same	Increase

23.2 GdO should be a slab-like, relatively unstable compound.

23.3 Increase the coordination number at Ln^{3+} .

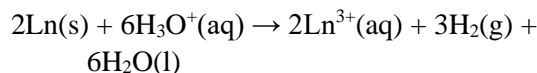
23.4 +6 (UO_2^{2+})

23.5



Exercises

23.1 a)



b) Most stable oxidation state for lanthanoids is +3

c) Ce and Eu.

23.2 The ionic radius of Lu^{3+} is significantly smaller than La^{3+} because of the incomplete shielding of the 4f electrons of the former.

23.3 They have easily accessible unusual oxidation states: Ce +4 and Eu +2.

23.4 Ln^{3+} cyclopentadienyl complexes exist in η^5 - η^1 equilibrium. The η^1 - Cp^- bonding mode can easily be substituted by another ligand, such as Cl^- . Larger U(III) triscyclopentadienyl complex does not have this equilibrium—all Cp^- rings are η^5 bonded and thus less labile.

23.5 Actinoids have a range of accessible oxidation states, just like d block metals.

23.6 UF_6 has a high degree of covalency, it is a molecular solid.

23.7 The composition of the solution can be complicated and could contain Pu(III), Pu(IV), Pu(V), and even Pu(VI) species because the potentials for the couples Pu(VI)/Pu(V), Pu(V)/Pu(IV), and Pu(IV)/Pu(III) are very similar. PuF_3 is likely to precipitate.

23.8 All these fragments are linear because this geometry maximizes the strong σ -overlap between 2p orbitals on the oxygen atoms and $6d_{z^2}$ and $5f_{z^3}$ orbitals on the An atom. Bond order is 3 for all species mentioned.

23.9 $\text{Tb}^{3+} \ ^7\text{F}_6$; $\text{Nd}^{3+} \ ^4\text{I}_{9/2}$, $\text{Ho}^{3+} \ ^5\text{I}_8$, $\text{Er}^{3+} \ ^4\text{I}_{15/2}$, $\text{Lu}^{3+} \ ^1\text{S}_0$.

23.10 a) correct

b) incorrect: Ln^{3+} ions exchange water molecules very rapidly

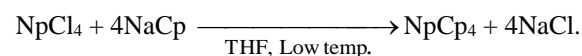
c) correct.

23.11 Apart from the fact that the discovery of a Ln(V) species would open a whole new avenue of chemistry, it would also shake the theoretical foundation of the claim that the lanthanide 4f subshell is rather inert. A good candidate could be Pr.

23.12 They share most stable oxidation states and half-filled orbitals.

23.13 For lanthanoids the 5d orbitals are empty, and the 4f orbitals are deeply buried in the inert [Xe] core and cannot participate in π -bonding.

23.14



23.15 The splitting of the 4f subshell by the ligands is negligible and does not vary as the ligands vary. The 5f orbitals of the actinoid ions interact more strongly with ligand orbitals, and the splitting of the 5f subshell, as well as the colour of the complex, varies as a function of ligand.

23.16 NaCl structure.

23.17 Os–O bond order is lower than 3 found in UO_2^{2+} .

Chapter 24

Self-tests

24.1 a) From SrCO_3 and TiO_2 in 1 : 1 ratio. The two are ground together and heated.

b) 3 : 2 stoichiometry (SrCO_3 : TiO_2); or from SrTiO_3 and SrO in 2 : 1 stoichiometry

c) Hydrothermal synthesis starting from $\text{Al}(\text{OH})_3$ and H_3PO_4 in the presence of a structure directing agent.

24.2 Because K^+ is a larger ion than Na^+ .

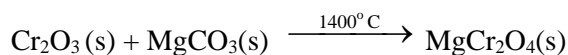
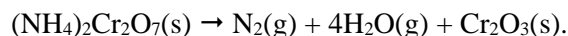
24.3 The A^{2+} ions (Fe^{2+} in this example) occupy tetrahedral sites and the B^{3+} ions (Cr^{3+}) occupy octahedral sites.

24.4 No; it lacks strongly acidic $\text{Al}-\text{OH}_2$ groups.

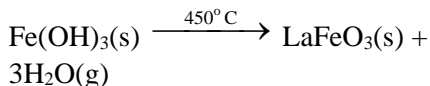
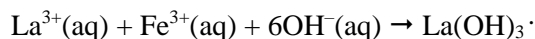
24.5 MCM-41.

Exercises

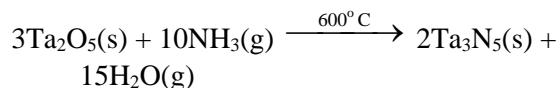
24.1 a)



b)

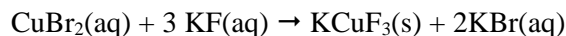


c)

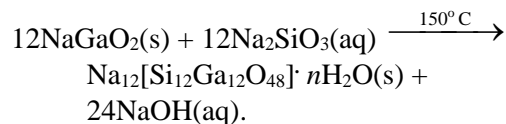


d) Heat an equimolar mixture of LiH and MgH_2 under inert atmosphere.

e)



f)



24.2 a) LiCoO_2 , b) Sr_2WMnO_6

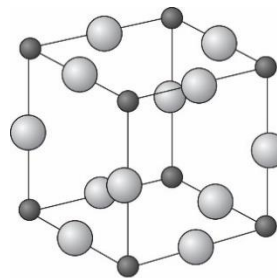
24.3 The electronic conductivity of the solid increases owing to formation of $(\text{Ni}_{1-x}\text{Li}_x)\text{O}$.

24.4 Fe_xO contains vacancies.

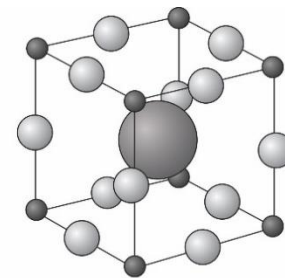
24.5 Using electron microscopy and X-ray diffraction.

24.6 a) Na^+ b) Ca^{2+} or Na^+

24.7 For the 1 : 1 Na:Re ratio the structure type can be described as that of perovskite (CaTiO_3).



ReO_3



Na_xReO_3

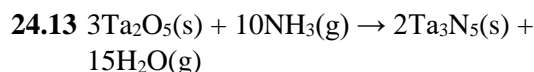
24.8 Fe^{3+} for B and $\text{Mo}(\text{VI})$ for B'.

24.9 Li^+ and possibly Na^+ .

24.10 Below 122 K.

24.11 ZnCr_2S_4 and NiLi_2F_4 .

24.12 All except compound c).



24.14 Formation of a glass is favoured for the substances that have polyhedral, corner-sharing oxygen atoms and that can retain the coordination sphere around a glass-

- forming element while having variable bond angles around O atom.
 CaF₂ is an ionic compound—on cooling, Ca²⁺ and F⁻ ions simply pack into the fluorite structure. SiO₂ has a framework structure composed of SiO₄ tetrahedra connected through O atoms shared at corners. The Si–O bond has significant covalent character and is very strong. This network is not easily broken (and reformed) with temperature.
- 24.15** BeO, B₂O₃, and to some extent GeO₂ are glass forming. Transition metal and rare earth oxides are typically non-glass-forming oxides.
- 24.16** Two tin fluorides and SbF₃.
- 24.17** (i) Direct combination of lithium and TiS₂ at elevated temperatures or (ii) electrointercalation.
- 24.18** Both [Co(η⁵-C₅H₅)₂] and [Co(η⁵-C₅Me₅)₂] are 19-electron species and can be easily oxidized to 18-electron species. Ferrocene is an 18-electron compound and cannot be easily oxidized.
- 24.19** The Mo₆S₈ units are bonded via Mo–S bridges. The S atoms in one cube donate an electron pair from a filled p orbital to the empty 4d_{z²} orbital on Mo located on a neighbouring cube.
- 24.20** Be, Ga, Zn and P.
- 24.21** (AlP)O₄, (BP)O₄ (ZnP₂)O₆
- 24.22** a) H₃O⁺ cations usually balance the charge
 b) Ga³⁺, Co³⁺ or Fe³⁺.
- 24.23** Only the reactants of appropriate size and shape can enter the zeolite structure. Similarly, only products of certain shape and size can exit the structure. Another way in which zeolite structure can control the outcome of the reaction is through transition-state selectivity: specific orientation (dictated by the pore/channel shape and size) of reactive intermediates determines the products of reaction.
- 24.24** Ambidentate ligands.
- 24.25** 10.6%, a good candidate but high temperatures required for decomposition.
- 24.26** Li_xMg_{1-x/2-2y/3}Al_yH_{2+z}, could be prepared from elements.
- 24.27** It easily decomposes and does not have a straightforward synthesis from the elements.
- 24.28** The Cu site in Egyptian blue is square planar and thus has a centre of symmetry; in copper aluminate spinel blue, the site is tetrahedral with no centre of symmetry.
- 24.29** In the solution an anionic radical S₃⁻ is present but is very sensitive to O₂ from the atmosphere; upon oxidation the colour is lost.
- 24.30** (i) High efficiency of light absorption (ii) efficient electron-hole separation process and (iii) high surface area of bulk material.
- 24.31** BN > C(diamond) > AlP > InSb.
- 24.32** In Na₂C₆₀, the tetrahedral holes are filled with sodium cations within the close-packed array of fulleride anions. In Na₃C₆₀, the tetrahedral holes and all of the octahedral holes are filled with sodium cations within the fcc lattice of fulleride anions.
- 24.33** a) 1.256 × 10³ nm² versus 1.256 × 10⁷ nm²
 b) 10 nm is a nanoparticle.
 c) A true nanoparticle should have a localized surface plasmon without characteristic momentum and of high intensity.
- 24.34** (a) Top-down: requires one to “carve out” nanoscale features from a larger object e.g. lithography. Bottom up: requires one to “build up” nanoscale features from

smaller entities e.g. thin film deposition of quantum wells.

b) Top-down methods allow for precise control over the spatial relationships between nanoscale entities, but they are limited to the design of rather large nanoscale items. Bottom-up methods allow for the precise spatial control over atoms and molecules relative to each other, but the long-range spatial arrangement is often difficult to realize.

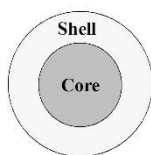
24.35 a) reacting species and additives must be solvated; stable nuclei of nanometer dimensions must be formed from solution; growth of particles to the final desired size.

(b) So that nucleation fixes the total number of particles and growth leads to a controlled size and a narrow size distribution.

(c) Stabilizers prevent unwanted Ostwald ripening.

24.36 Smaller particles present in the solution dissolve and this redissolved material precipitates again but on the surface of existing particles.

24.37 a)



b) i) Solution based: grow the core in solution and add the additive and material for the growth of shell. ii) Vapor-deposition: deposit the material for the core and then the material for the shell.

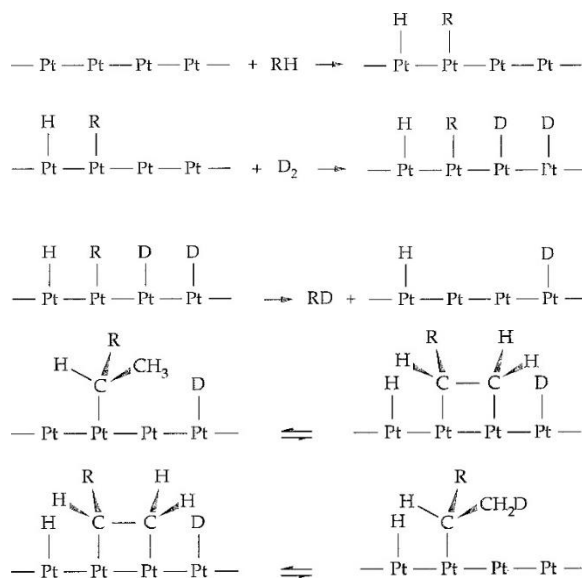
c) Biosensing.

24.38 Hexagonal BN, sheet silicates and molybdenum sulfide.

24.39 A thin foil of platinum-rhodium will not have as much surface area as an equal

amount of small particles finely dispersed on the surface of a ceramic support.

24.40



24.41 Pt has a strong tendency to chemisorb CO.

24.42 Electrocatalysts are compounds that are capable of reducing the kinetic barrier for electrochemical reactions (barrier known as overpotential).

Chapter 25

Self-Tests

25.1 40, pharmaceutical industry

25.2 33.4%

25.3 31%.

25.4 Ir catalyst does not have side reactions.

Exercises

25.1 3.5

25.2 7.

- 25.3** yield 80%, atom economy 25.9%; good yield poor atom economy.
- 25.4** yield 63%, atom economy 79%; both are acceptable but could be better.
- 25.5**
- Amount of the product formed per unit time per unit amount of the catalyst used.
 - A measure of how much of the desired product is formed relative to undesired by-products.
 - A substance that increases the rate of a reaction but is not consumed itself.
 - A sequence of chemical reactions involving the catalyst that transform the reactants to product(s).
 - A solid surface over which the solid state catalyst is finely divided.
- 25.6** HI hydrolyses MeCOOMe and produces MeI and MeCOOH (instead of water).
- 25.7** Hazard refers to anything that could pose a harm to people, property or the environment. Risk is a measure of probability the hazard will do harm.
- 25.8** The safety principle is consideration of safety of a reaction, process or design by bearing in mind known hazards and risks associated with them.
- 25.9** Real-time, in-process monitoring provides timely information on a reaction's progress, state of a catalyst, formation of any by-products, etc. This information can alert to any problems that arise during the process and thus help in prevention of serious accidents to people, property or the environment.

Chapter 26

Self-Tests

- 26.1** No.

- 26.2** The protein's tertiary structure can place any particular atom or group in a suitable position for axial coordination.
- 26.3** If a patient was given an intravenous fluid containing KCl instead of NaCl, the potential across the cell membrane would collapse, with severe consequences.
- 26.4** As the Ca^{2+} concentration increases in the cell, the Ca-calmodulin complex is formed. The binding of this Ca-calmodulin complex to the pump is thus a signal informing the pump that the cytoplasmic Ca^{2+} level has risen above a certain level and to start pumping Ca^{2+} out.
- 26.5** Starting from a Fe(II) porphyrin complex (L is a neutral axial ligand throughout the sequence) we first obtain a peroxo bridged Fe(III) porphyrin dimer. Peroxo bridge can oxidatively cleave producing two equivalents of oxido Fe(IV) porphyrin monomers. This rather reactive species can react with another equivalent of the starting Fe(II) porphyrin complex producing an oxido-bridged Fe(III) porphyrin dimer.
- 26.6** Hydrogen bonding and replacement of one cysteine with a histidine should lead to an increase in the reduction potential of an Fe-S cluster.
- 26.7** There is greater covalence in blue Cu centres than in simple Cu(II) compounds.
- 26.8** Likely to be highly oxidizing, and probably diamagnetic with a preference for square-planar geometry.
- 26.9** The way to obtain a better model for Fe(IV) oxo centres is to force the octahedral geometry at Fe(IV). For non-haem Fe proteins the ligands should contain N and O donor atoms.
- 26.10** Cobalamins can produce species such as CH_3Hg^+ and $(\text{CH}_3)_2\text{Hg}$ that are

hydrophobic and can penetrate cell membranes.

26.11 Spectroscopic measurements that are metal specific, such as EPR, could be used on both enzyme and isolated cofactor. Attempts could be made to grow single crystals from the solution and perform single-crystal X-ray diffraction and EXAFS to reveal molecular geometry, bond distances, and angles between Fe or Mo and the sulphur ligands.

26.12 Cu(I) has an ability to undergo linear coordination by sulfur-containing ligands.

Exercises

26.1 For a channel or ionophore to be Na⁺ specific it must have smaller cavity than K-channel. Ca²⁺ is going to bind more tightly than either Na⁺ or K⁺ to the residues that have negative charge. It is a cation of a s-block element and has no LFSE that could dictate a preferred geometry. Cl⁻ is obviously different from the other three by being an anion. Thus, to move Cl⁻ we would need to have a large cavity and rely on hydrogen bonds formed with -NH and -OH functional groups.

26.2 The larger size of lanthanides is compensated for by their higher charge, although they are likely to have higher coordination numbers.

26.3 Co(II) commonly adopts distorted tetrahedral and five-coordinate geometries typical of Zn(II) in enzymes. When substituted for Zn(II), the enzyme generally retains catalytic activity. Co(II) is a d⁷ cation, and its peaks in the UV-Vis spectrum are quite intense.

26.4 Acidity of coordinated water molecules is in the order Fe(III) > Zn(II) > Mg(II).

Ligand-binding rates are Mg(II) > Zn(II) > Fe(III).

26.5 Either EPR or Mössbauer spectroscopy.

26.6 The two central lines correspond to Fe³⁺. The two new ones show a larger quadrupole coupling and a higher isomer shift, characteristics consistent with high-spin Fe²⁺. Since the signals from Fe²⁺ and Fe³⁺ in the reduced form are well separated, there is no delocalization.

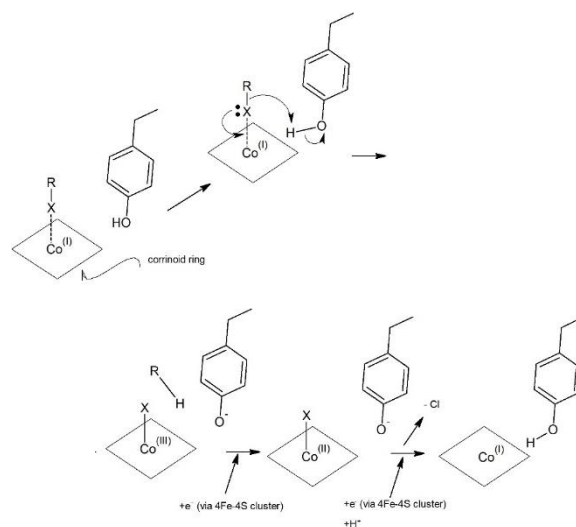
26.7 The change in structure suggests that the coupling of proton and electron transfer can also occur at the P-cluster by controlling protonation of the exchangeable ligands.

26.8 Co(I) and Co(III); Fe(II) or Zn(II).

26.9 Would indicate the presence of photosynthesis and consequently some life-form that is capable of photosynthesis.

26.10 EPR spectroscopy; use of isotopically labelled water molecules, for example H₂¹⁷O, can be combined with Raman and IR spectroscopies.

26.11



Chapter 27

Self-Tests

27.1 By modifying R substituents (R^1 – R^5) on the ligand backbone.

Exercises

27.1 Both have a preference for square planar geometry that seems to be necessary for the activity of Pt(II) anticancer drugs. Au(III) is also a soft Lewis acid, meaning that it has low preference for Cl^- and O-donor ligands. The major difference is that Au(III) is easily reduced under hypoxic conditions to Au(I), which prefers linear geometry as in $[AuCl_2]^-$.

27.2 Copper slowly oxidises in air producing copper oxides. The epidermis is slightly acidic, meaning a small amount of the oxide can dissolve to produce Cu^{2+} , which is water soluble and can pass through the skin.

27.3 $B(OH)_3$, H_2 , CO , and OH^- . In neutral or mildly acidic medium it would be protonated to produce hydrogenboranocarbonate that can eliminate OH^- to produce $[H_3BCO]$ adduct. Then CO can be easily displaced by water molecules. The intermediate aquo adduct $[H_3B(OH_2)]$ rapidly decomposes to give H_2BOH and H_2 . H_2BOH reacts rapidly with another two water molecules to produce the final products $B(OH)_3$ and two more equivalents of H_2 .

27.4 Choose a trace element (not CHNOPS); list what its important chemical properties are, including aqueous chemistry, redox chemistry; identify proteins in which such an element appears; discuss how the element's chemical properties suit it for its task.

27.5 Gallium(III) can bind to transferrin and lactoferrin, and can even be incorporated into ferritin. These enzymes use nitrogen and oxygen donors to bind iron. Since Ga(III) also has a good affinity for the same donors, it can compete with Fe(III) for the binding sites.

27.6 In the strongly acidic environment (pH ~ 3) that abounds in organic acids, Bi(III) compounds form polymeric species and clusters that can form a protective layer (or coating) on the stomach.